REACTION KINETICS OF NOVEL EMULSIFIED ACID SYSTEM WITH LIMESTONE

BY

MUSA ELTAYEB MUSA AHMED

A Thesis Presented to the
DEANSHIP OF GRADUATE STUDIES

KING FAHD UNIVERSITY OF PETROLEUM & MINERALS

DHAHRAN, SAUDI ARABIA

In Partial Fulfillment of the
Requirements for the Degree of

MASTER OF SCIENCE

In

PETROLEUM ENGINEERING

June, 2017

KING FAHD UNIVERSITY OF PETROLEUM & MINERALS

DHAHRAN- 31261, SAUDI ARABIA

DEANSHIP OF GRADUATE STUDIES

This thesis, written by **MUSA ELTAYEB MUSA AHMED** under the direction of his thesis advisor and approved by his thesis committee, has been presented and accepted by the Dean of Graduate Studies, in partial fulfillment of the requirements for the degree of **MASTER OF SCIENCE IN PETROLEUM ENGINEERING.**

Dr. Abdullah Sultan
(Advisor)

Dr. Dhafer Al Shehri
Department Chairman

Prof. Sidqi Ahmad M Abu-Khamsin
(Member)

Dr. Salam A. Zummo
Dean of Graduate Studies

Dr. Dominic Brady
(Member)

14/9/17
Date

31/8/2017

Dedication

I dedicate this effort to my beloved parents, brothers, sisters and fiancée

ACKNOWLEDGMENTS

Firstly, I would like to thank Almighty Allah for giving the power, strength, and passion for completing my MS Thesis work. without his care, I couldn't have done anything. Thank you, Allah, for every single blessing that covers me.

I am extremely thankful to King Fahd University of Petroleum & Minerals for the scholarship that I have awarded to peruse my Master's program.

My deep gratitude goes to my advisor Dr. Abdullah Sultan for the continuous support of my MS study and research, for his enthusiasm, patience, guidance, motivation, and immense knowledge. His advice helped me in all the time of research.

Also, I would like to express my sincere appreciation to my thesis committee members, Dr. Dominic Brady and Prof. Sidqi Ahmad M Abu-Khamsin for their encouragement, insightful comments, and suggestions.

I would also like to convey my gratitude to the Center for Integrative Petroleum Research (CPIR) at the College of Petroleum Engineering and Geoscience for providing me with the lab access to conduct the first part of my research. I want to thank CPIR people, Ahmad Adewunmi, Dr. Jimoh Adewole, Abdelmlik Elsnona, and Abdelrhman Algamdi who helped me a lot during my work at RI.

Special thanks to my colleagues Ziad Soidoui and Khaled Zidan from whom I learned how to conduct RDA experiments and emulsified acid preparation.

In addition, I would like to appreciate Schlumberger Dhahran Carbonate Research Center (SDCR) for providing access for performing experimental work there. An exceptional acknowledgment to Xiangdong Qiu who helped and guided me greatly throughout the second part of my work conducted at SDCR. In addition, Nadir Othaibi, also helped me a lot in conducting the coreflood experiments at SDCR.

TABLE OF CONTENTS

ACKNOWLEDGMENTS ..... **V**

TABLE OF CONTENTS ..... **VII**

LIST OF TABLES ..... **X**

LIST OF FIGURES ..... **XI**

ABSTRACT ..... **XIII**

ملخص الرسالة ..... **XV**

CHAPTER 1 INTRODUCTION **1**

1.1 Background **1**

1.2 Emulsified Acid **5**

1.4 Problem Statement and Research Objectives **8**

CHAPTER 2 LITERATURE REVIEW **10**

2.1 Reaction Kinetics of HCl with Calcite **10**

2.2 Reaction Kinetics of HCl with Dolomite **13**

2.3 Reaction Kinetics of Gelled Acid with Calcite **14**

2.4 Reaction Kinetics of Emulsified Chelating Agent with Calcite **15**

2.5 Reaction Kinetics of Organic Acid with Calcite **16**

2.6 Reaction Kinetics of Organic Acid with Dolomite **16**

2.7 Reaction Kinetics of Emulsified Acid with Calcite **17**

2.8 Reaction Kinetics of Emulsified Acid with Dolomite **19**

CHAPTER 3 RESEARCH METHODOLOGY **23**

3.1 Materials **23**

3.1.1 Diesel 23

3.1.2 Waste Oil 23
3.1.3 Hydraulic Acid 23
3.1.4 Emulsifier 24
3.1.5 Nanoclays 24
3.1.6 Calcite Disks 24
3.1.7 Indiana Limestone Cores 24
3.1.8 Crude Oil 24
3.2 Equipment 25
3.2.1 Rotating Disk Apparatus 25
3.2.2 Dual Coreflood System 27
3.2.3 ICP-OES 27
3.2.4 Toshiba Medical CT-Scanner Machine 31
3.2.5 High Shear Mixer 31
3.2.6 Dosimeter 31
3.2.7 Conductivity Meter 31
3.2.8 Oven 35
3.2.9 Helium Porosimeter 35
3.2.10 Weighing Balance 35
3.2.11 X-ray Diffraction 35

3.3 Methodology 38
3.3.1 Diesel Emulsified Acid preparation 38
3.3.2 Waste oil emulsified acid preparation 39
3.3.3 Rotating disk experiment setup and procedures 40
3.3.4 Core-Flood Experiment Setup and Procedures 41

3.4 Rotating Disk Theory 41

CHAPTER 4 CORE FLOOD EXPERIMENTS RESULTS 57

4.1 Core Flood Study 57

4.2 Basic Analysis description 58

4.3 Stability of Emulsified Acids at 135°C 59

4.4 Pressure Drop Profiles 61

4.5 Optimum Injection Rate 64

4.6 Inlet Face Image of the Cores 67

4.7 CT Scan for Acidized Cores 67

CHAPTER 5 ROTATING DISK EXPERIMENT RESULTS 72

5.1 XRD and XRF Analysis of Calcite Core 72

5.2 Viscosity of Emulsified Acids at a Temperature of 135°C 75

5.3 Stability of Emulsified Acids at a Temperature of 135°C 77

5.4 Reaction of Emulsified Acid and Limestone 79

5.5 Emulsified Acid - Limestone Surface Reaction Pattern 80

5.6 Calculation of Emulsified Acid- Limestone Dissolution Rate: 82

5.7 Diffusion Coefficient of Emulsified Acid with Dry and Oil Saturated Limestone. ... 86

CHAPTER 6 88

CONCLUSIONS AND RECOMMENDATIONS 88

Conclusions 88

Recommendations 89

REFERENCES 91

VITAE 95

LIST OF TABLES

Table 2. 1 Reaction kinetics literature review summary 1 20

Table 2. 2 Reaction kinetics literature review summary 2 21

Table 2. 3 Reaction kinetics literature review summary 3 22

Table 3. 1 Sara analysis for the crude oil 25

Table 4. 1 Core flood experiment schedule 58

Table 5. 1 XRF results 73

Table 5. 2 Power-low values at different temperature for the emulsified acid 75

Table 5. 3 Set # 1 Experiment Parameters 79

Table 5. 4 Set # 2 Experiment Parameters 80

Table 5. 5 The values for the function $\emptyset(\boldsymbol{n})$ at different power-law indices 86

LIST OF FIGURES

Figure 3. 1 Rotating disk apparatus 26

Figure 3. 2Dual core flood system 29

Figure 3. 3 ICP-OES 30

Figure 3. 4 Toshiba CT scan machine 32

Figure 3. 5 High shear mixer 33

Figure 3. 6 Dosimat 34

Figure 3. 7 Conductivity meter 34

Figure 3. 8 Helium Porosimeter 36

Figure 3. 9 XRD equipment 37

Figure 4. 1 Waste oil emulsified acid stability at 135°C 60

Figure 4. 2 Diesel emulsified acid stability at 135°C 60

Figure 4. 3 Pressure drop profile for waste oil emulsified acid coreflood experiments ... 63

Figure 4. 4 Pressure drop profile for diesel emulsified acid 63

Figure 4. 5 Pore volumes injected to achieve breakthrough at different injection rate 66

Figure 4. 6 Inlet face images for all cores 69

Figure 4. 7 3D CT Scan for acidized cores analyzed through Pregeos software 70

Figure 4. 8 Wormhole volume fraction along the core for diesel emulsified acid 71

Figure 4. 9 Wormhole volume fraction along the core for waste oil emulsified acid 71

Figure 5. 1 XRD results for calcite disks used in this study 74

Figure 5. 2 The power low constant correlation with temperature 76

Figure 5. 3 The power low index correlation with temperature 76

Figure 5. 4 Stability of Emulsified Acids at a temperature of 135°C 78

Figure 5. 5 Stability of Emulsified Acids at a temperature of 135°C 78

Figure 5. 6 Emulsified acid - limestone surface reaction pattern 81

Figure 5. 7 Calcium concentration with time for dry limestone reaction kinetic at different RPM 83

Figure 5. 8 Calcium concentration with time for crude oil saturated limestone at different rpm. 83

Figure 5. 9 The F-function versus disk rotational speed to the power 1/(1+n)..... 85

ABSTRACT

Full Name : Musa Eltayeb Musa Ahmed

Thesis Title : Reaction Kinetics of Novel Emulsified Acid with Limestone

Major Field : Petroleum Engineering

Date of Degree : June 2017

Emulsified acids have been used as an effective well stimulation fluid since 1933. It is primarily an emulsion solution consisting of two immiscible liquids, one of them is dispersed (inner or dispersed phase) in the other liquid (continuous or outer phase) in the form of droplets. Recently, waste oil as a continuous phase was proposed as a cheap alternative to diesel and other expensive hydrocarbons when formulating emulsified acid. The new acid system rheology and stability was addressed in several publications, however, the reaction kinetics of this novel acid system was not considered and hence this study to fill the gap. Furthermore, most of the reaction kinetics for the conventional diesel emulsified acid was done at relatively Low pressure and temperature LPLT without taking into account the effect of crude oil saturation, therefore, this issue is also, examined through this study.

The first part of this work, study the feasibility of waste oil emulsified acid system (novel) in acid stimulation treatment. In particular, emulsion stability, and reactivity (reaction kinetics) with limestone reservoir rock at high-pressure high-temperature HPHT were investigated. The reactivity was carried out through a series of core flow experiments at HPHT and compared with another one done using the conventional diesel emulsified acid.

From the lab work and results The new waste emulsified acid system showed good potential as stimulation fluid compared to both diesel and plain HCl. For instance, the new acid system achieved the lowest pore volume of acid to break through (PVBT) among the three stimulating fluids i.e (Waste, Diesel, and plain HCl).

In the second part of the work, the reaction kinetics (Diffusion coefficient) of diesel emulsified acid with limestone at HPHT has studied as well as the effect of crude oil saturation on these reactions. The effect is studied through Rotating Disk Apparatus RDA experiments. All the experiments were conducted at HPHT that mimics the real reservoir conditions for emulsified acid stimulation.

From the last part results a couple of two conclusions were drawn, firstly the Diffusion coefficient (D_e) value at HPHT is much lower than those obtained at LPLT and the extrapolation of these D_e values at lower down hole conditions for deep reservoirs could lead to severe acidizing and hydraulic fracturing design inaccuracy. Secondly, interestingly two D_e values were reported for oil saturated limestone reaction kinetics and this mainly because of crude oil saturation effect.

ملخص الرسالة

الاسم الكامل: موسى الطيب موسى احمد

عنوان الرسالة: دراسة حركية التفاعلات الكيمائية لمستحلب حمض جديد مع صخر الحجر الجيري(كالسايت)

التخصص: هندسة البترول

تاريخ الدرجة العلمية: يونيو2017

مستحلبات الاحماض استخدمت كسوائل تحسين فعالة لآبار النفط منذ عام 1933. مستحلب الحمض هو في المقام الأول محلول مستحلب يتكون من اثنين من السوائل غير قابلة للامتزاج، واحد منهم مشتت (الطور الداخلي-الطورالمشتت) في السائل الآخر (الطور الخارجي-الطور المستمر) في شكل قطيرات. في الآونة الأخيرة، اقترحت مخلفات الزيوت لتستخدم كطور مستمر و كبديل رخيص للديزل وغيرها من الهيدروكربونات غالية الثمن عند تكوين حمض مستحلب. تم تناول دراسة اللزوجه الاستقرارية لمستحلب الحمض الجديد في العديد من المنشورات، ولكن لم يتم النظر في حركية تفاعل هذا النظام الحمضي مع الصخور، وبالتالي هذه الدراسة لملء هذا الفراغ. علاوة على ذلك، كان معظم دراسات حركية التفاعل للاحماض المستحلبة تجرى في ظروف ضغط وحرارة منخفضتين نسبيا,ودون الأخذ بعين الاعتبار تأثير تشبع النفط الخام للصخور، لذا سيتم فحص هذه المسألة، من خلال هذه الدراسة. الجزء الأول من هذا العمل، يدرس مدي جدوى الحمض المستحلب الجديد في عملية تطوير آبار النفط. على وجه الخصوص، تم دراسة استقرارية الحمض المستحلب الجديد، وكذلك حركية التفاعل مع مكامن الحجر الجيري (كالسايت) عند ضغط وحرارة مرتفعتين. وقد أجريت التفاعلات من خلال سلسلة من تجارب السريان في العينات الصخرية الأساسية في ظروف ضغط وحرارة مرتفعتين ومقارنتها مع واحدة أخرى اجريت باستخدام مستحلب الحمض التقليدي المكون من الديزل.

من عمل المختبر والنتائج أظهر نظام الحمض المستحلب الجديد إمكانيات جيدة كسوائل تحسن للابار مقارنة بكل من مستحلب الديزل وحمض الهيدروكلوريك. على سبيل المثال، حقق النظام الحمضي الجديد أقل حجم لاختراق الصخرة مقارنة بحمض الهيدروكلورك العادي وكذلك مستحلب الديزل.

في الجزء الثاني من العمل، تم دراسة حركية التفاعل (معامل الانتشار) من حامض الديزل المستحلب مع الحجر الجيري

عند ضغط وحرارة مرتفعتين وكذلك تاثير تشبع النفط الخام للصخور على هذه التفاعلات. تم دراسة هذا التأثير من خلال مجموعة من التجارب باستخدام جهاز القرص الدوار. أجريت جميع التجارب في حرارة وضغط عاليين تشابه الحالة الحقيقية لمكمن النفط.

من نتائج الجزء الأخير تم استخلاص اثنين من الاستنتاجات، أولا قيمة معامل الانتشار (D_e) عند الضغط والحرارة المرتفعين أقل بكثير من تلك التي تم الحصول عليها عند قيم اقل من الحرارة والضغط. أستخدام قيم معامل الانتشار المستخلصة عند درجات حرارة وضغط منخفضتين قد تودي الي خطا كبير عند تصميم عمليه تحسين الابار لمكامن ذات اعماق عالية. ثانيا، من المثير للاهتمام انه و على عكس السائد وجد ان هناك قيمتين لمعامل الانتشار عند دراسة حركية تفاعلات مستحلب النفط مع الحجر الجيري وذلك عندما يتم التشبيع للصخور بالنفط.

CHAPTER 1
INTRODUCTION

1.1 Background

The ultimate goal of well stimulation is enhancing the connection between a well and a reservoir by eliminating formation damage near the wellbore and therefore, ease the movement of fluids that are injected or produced from the formation. Formation damage is an inevitable process that happens in the wellbore and causes the productivity or injectivity to decline. Formation damage can occur as side effects from drilling operations, like mud solids invasion, completion, like poor perforation, production, like asphaltenes deposition, and others (Economides and Nolte 2000). Also, well stimulation practices are used to improve the near-wellbore region in cases of tight zones or to extend connections between created perforations and reservoir, i.e. carbonates acidizing. For decades, well stimulation acquired significant attention and interest for petroleum industry's researchers, engineers, and operators, and extensive research and efforts took place to develop and improve methods to enhance wells performance and increase the profit. Production engineers seek constantly for better ways to increase recovery from oil and gas fields. Any successful stimulation project requires a thorough understanding of mechanisms by which fluids are flowing between reservoir and well and accurate assessment for the origins of declining well performance.

Well stimulation techniques can be broadly classified into acid fracturing, hydraulic fracturing, and matrix acidizing (Economides and Nolte 1989). In hydraulic fracturing, a

fluid is injected into the well at a pressure exceeding the breakdown pressure of the formation in order to create cracks or fractures propagating into the formation. During the process, a proppant is added to the injection fluid to precipitate inside the created fractures and hold pathways between well and formation. Hydraulic fracturing is preferred for tight sand formation where the permeability is too low. Acid fracturing is a hydraulic fracturing except that instead of using proppants in the injection, acid is used as the fracture fluid (Schechter 1992). The acid works on etching the fractures to make them longer. The technique of hydraulic fracturing was first introduced in oil industry during the 1940s, and since then, it was implemented in thousands of fields around the world with a satisfactory degree of success to help to recover massive amounts of gas and oil trapped in tight sands and unconventional reservoirs (Economides and Nolte 2000).

Matrix acidizing is the method of injecting acidic fluids into the surrounding formation below its fracturing pressure in order to dissolve damaged particles if the formation is sandstones or create new flow passages, in the case of carbonates formation, in order to increase the permeability around the wellbore. For a successful acidizing treatment to be achieved, several phases must be remembered and done properly, candidate selection, formation damage characterization, treatment selection and design, job execution and post-treatment evaluation. For all well stimulation operations worldwide, it's estimated that 80% of them are matrix acidizing treatments (Economides and Nolte 2000). Enhancement of production using acids is considered the best in terms of immediate productivity improvement and economic returns at a reasonable price (Zhang and Curran 2006).

The year 1895 witnessed the first treatment of acidizing when The Standard Oil Company used HCL to stimulate wells producing from carbonate formation in Ohio, USA (Williams

1979). Formation acidizing precedes all techniques of well stimulation ever existed in the industry. The first acidizing patent was issued to Herman Frasch, the chief chemist at The Standard Oil Company, on March 1896. Frasch's patent contained many elements that are being used in today's acidizing practices. In his patent, Frasch proposed a hydrochloric acid solution with 30 to 40% of HCl weight. His ideas turned out to be successful and resulted in creating wormholes in a limestone formation. Therefore, he was the inventor of acidizing. However, hydrochloric acid acidizing started to be used commercially in 1932 when great development occurred in dealing with corrosion problems caused by HCl. Acetic Acid, which is less corrosive than HCl, was introduced to the industry by Harris in 1961 and was used in some situations, particularly at high temperatures. Acetic Acid was less corrosive than HCl and could replace it in some applications. Shortly thereafter, Formic Acid got into the acidizing business and solved some problems associated with HCl acidizing. Development's history of sandstone acidizing started with a failure. In 1933, Halliburton Company used a mixture of hydrochloric acid (HCl) and hydrofluoric acid (HF) to treat a well drilled in a sandstone formation. This attempt resulted in substantial sand production into the wellbore. In the same year, Jesse Russel Wilson of the Standard Oil Company filed a patent for acidizing sandstone rock formation using HF acid (Wilson 1935). In his description of the problem, he mentioned that using a suitable reagent like hydrofluoric acid could dissolve materials that resulted in clogging up the pores or passages for flow. Later on, a mixture contained 3% HF and 12% HCl, known as regular-strength mud acid, became the desired option for treating sandstone formation. Following studies concerned with the development of an acid solution that is capable of retarding HF reaction for deeper acid penetration, preventing precipitation of HF/rock reaction products,

avoiding excessive acid reaction and stabilizing fine particles which are able to migrate and cause pore plugging (Kalfayan 2008).

Matrix acidizing falls into two categories, sandstone acidizing and carbonate acidizing. In sandstone acidizing treatments, the goal is to remove and dissolve damaging particles and debris that block flowing pores and passages in the rock matrix. Damage particles in near wellbore area may be naturally occurring or introduced by well operations. Therefore, sandstone acidizing is primarily a damage-removal process. Sandstone acidizing has a chance of success only in the presence of formation damage in the targeted area. Treating undamaged formation may not increase production significantly, except for certain cases like naturally fractured formation. Generally, the operation is performed by injecting three fluids in sequence. A preflush, which is usually 5-15% strength of HCl in addition to some additives, is used to displace connate water from near wellbore region. Then, a mixture of HF and HCl (with 3% and 12% respectively) is injected next to react and remove the damage. Finally, the after flush that could be HCl solution, hydrocarbon or gas, depending on the type of the well, is injected. Acids commonly used in sandstones are hydrochloric, hydrofluoric, acetic and formic acid (Kalfayan 2008; Schechter 1992).

The main task in acidizing carbonate rocks is to improve the flow capability by creating conductive passages, called wormholes, which penetrate into the rocks and bypass the damage. Two major types of carbonate rocks are generally treated by acidizing, dolomite and limestone. Dolomite minerals are primarily formed of calcium magnesium carbonate ($CaMg(CO_3)_2$), where limestone minerals are collected largely of calcium carbonate ($CaCO_3$). Hydrochloric acid is the most common acid used in acidizing applications in the industry for several reasons. It is cheap and available, it is powerful in dissolving the rock,

and its reaction with carbonate rocks is very rapid. However, it's highly corrosive. It has a low viscosity which prevents good wellbore coverage, therefore, lead to ineffective results. Also, its high reactivity with the rock provides no deep penetration in the formation (Buijse and Van Domelen 2000; Economides and Nolte 2000; Kalfayan 2008). The reaction of HCl with both calcite and dolomite respectively is represented as follows:

$$2HCl + CaCO_3 \rightarrow CaCl_2 + CO_2 \uparrow + H_2O$$

$$4HCl + CaMg(CO_3)_2 \rightarrow CaCl_2 + MgCl_2 + 2CO_2 \uparrow + 2H_2O$$

The reaction occurs in three basic steps: (1) diffusion of hydrogen ion to the rock surface, (2) rock surface reaction, and (3) reaction products (Ca^{2+} and Mg^{2+}) diffusion back to the solution (S. H. Al-Mutairi et al. 2008).

There are other types of acids used frequently in carbonates acidizing such as gelled acids, emulsified acids, micro emulsions, organic acids and viscoelastic surfactant-based (VES) acids. The type of acid used affects the shape and extension of created wormholes. Strong acids, such as HCl, tend to produce single wormholes without branching, whereas weaker acids, such as acetic acid, and retarded acid systems, such as emulsified acid and gelled acid create more branching of wormholes.

1.2 Emulsified Acid

Emulsified acid is primarily an emulsion solution consisting of two immiscible liquids, one of them is dispersed (inner or dispersed phase) in the other liquid (continuous or outer phase) in the form of droplets. The inner phase usually contains a hydrochloric acid solution and corrosion inhibitor, when needed. The outer phase consists of hydrocarbon

fluid, diesel usually, and emulsifier. Because emulsified acid is thermodynamically unstable, the emulsifier is brought to stabilize the system by reducing the interfacial tension between the two liquids to a degree that allows them to mix and form one stable mixture (S. H. Al-Mutairi et al. 2008). The outer phase acts as a barrier between acid and tubular to protect them against corrosion. The intention that stands behind the extensive use of emulsified acid in the industry can be concluded in the following points:

1. It is known that HCl solution is highly corrosive to the steel parts in the well. The physical characteristics of the emulsified acid where the acid is placed in the dispersed phase minimize the danger of corroding and damaging the tubular.

2. HCl reaction with the rock is very rapid. In many cases, the reaction takes place without achieving the desired enhancement in the surrounding formation. The emulsified acid tackles this problem with its retardation property. By this, emulsion solution is able to be pumped deep into the formation to cover the region and then reacts to accomplish the effect needed.

3. The high viscosity of the emulsified acid allows it to sweep the targeted region and distribute uniformly.

The emulsified acid was first introduced for the industry through a patent granted to Melvin de Groote, an American chemist, in 1933 (De Groote 1933). In his procedure for making the emulsion, he used HCl and nitric acid and used crude oil with other liquids as the continuous phase. Sulfonic acid was introduced as an emulsifying agent. In the first place, De Groote's aim to invent this acid system was to tackle the corrosion problem associated with using straight HCl acid in acidizing treatments; this problem could limit the benefit

of the treatment process. Emulsified acid basically created to act as a corrosion inhibitor (S. H. Al-Mutairi, Hill, and Nasr-El-Din 2007). Since then, emulsified acids are widely used in carbonate fracturing and matric acidizing.

Emulsified acid has three important properties needed to be considered in its design and application: stability, rheology, and reactivity. The emulsion has to be stable enough during its injection and never break before it penetrates deep into the formation. High downhole temperatures pose a challenge because as the temperature increases the emulsion becomes less stable, which may lead to failure of the treatment. For the emulsified acid rheology, the viscosity is an important feature. Increasing the emulsion viscosity can result in better zonal coverage that leads to improved permeability enhancement, especially in heterogeneous formation. In addition, as the emulsion becomes more viscous, it becomes more stable as well. However, the high viscosity of the emulsion poses high friction pressure during pumping. After the breaking of the emulsion, the reaction between acid and rock takes place as that of plain HCl with calcite or dolomite. For emulsified acid reaction with carbonates, the hydrogen ion does not diffuse directly in the continuous phase. Therefore, the process of the reaction, mentioned above, will also include (1) the diffusion of acid droplets in the continuous phase; and (2) the breakup of the acid droplets before they react with the calcite surface (S. H. Al-Mutairi et al. 2008).The retardation feature of emulsified acid makes its reaction with formation rock lower than that of plain HCl.

All of the characteristics of emulsified acids highlighted in the previous paragraph are influenced by several parameters such as emulsifier concentration, acid’s droplet size, the

viscosity of the emulsion, acid concentration, downhole conditions, rocks mineralogy, type of fluid used as the continuous phase etc.

1.4 Problem Statement and Research Objectives

Having reviewed the previous research and studies related to emulsified acids application in well stimulation it has understood that the emulsified acid is an effective tool in performing the acidizing job.

The common two problems with emulsified acid are the stability with temperature and it economical cost. Currently, oil industry uses emulsified acid which contains 30 vol.% diesel and 70 vol.% acid. Although this emulsion satisfied the technical objectives required it is too expensive stimulation fluid. Another issue is that most of the emulsifiers used in these emulsified acids are not stable at high temperature.

Recently, waste oil emulsified acid showed a good potential as stimulation fluid (Sidaoui et al. 2016) (Sidaoui, Sultan, and Brady 2017) in term of rheology and stability, however, it is reactivity with reservoir rock wasn't studied.

Based on the literature review the following conclusions can be drawn:

I. Previous work did not include the effect of high pressure on the reaction rate of emulsified acid of dolomite and limestone cores

II. Currently, oil industry relatively uses an expensive emulsified acid which contains 30 vol. % diesel and 70 vol. % acid.

III. Most of the rotating desk experiments have been done on the dry core which does not represent the actual field condition.

IV. Waste oil emulsified acid (The novel emulsion) Reaction kinetics has not studied.

A novel emulsified acid system is proposed, in this thesis work. In order to model the carbonate acidizing treatment of the new novel emulsified acids the reaction kinetics between the petroleum reservoir rock and these systems should be known. These reaction kinetics studies will estimate the important experimental parameters that required in carbonate acidizing modelings such as the diffusion coefficient and the optimum injection rate, those parameters are commonly driven from Rotating Desk Apparatus and coreflood experiments using the selected stimulating fluid and rock sample that represent the reservoir.

The objectives of this work:

1. Evaluate the reactivity of the new emulsified acid (Waste oil emulsified acid) system with limestone.
2. Study the reaction kinetics of diesel emulsified acid at HPHT.
3. Investigate the effect of oil saturation on the emulsified acid and limestone reaction kinetics.

CHAPTER 2

LITERATURE REVIEW

2.1 Reaction Kinetics of HCl with Calcite

It is commonly known that the reaction of HCl with calcite is much faster than that with dolomite. (Lund et al. 1975) used the rotating disk apparatus RDA to study the dissolution of calcite with hydrochloric acid. Experiments were conducted at 800 psig, a temperature range of -15.6– 25°C, acid concentration 0.1– 9 N and disk rotational speed 100 –500 rpm. It was reported that at 25°C, the reaction is limited by mass transfer even at the relatively high rotational speed of 500 rpm whereas, at -15.6°C both the surface reaction and mass transfer rate was reported to limit the dissolution rate of calcite. In conclusion, the result of this study cannot be used to simulate the real field conditions since all the experiments were conducted at relatively low pressure and temperature.

(K. C. Taylor, Mehta, and Aramco 2006) made a set of more than 60 experiments to measure the effect of acidizing common additives on both HCl-calcite and HCl-dolomite marble dissolution rate, using rotating disk apparatus RDA. Acids with a surfactant, polymer, quaternary amines, iron-chelating additives, mutual solvent and dissolved iron were used in this study. Desk rotational speed was 100, 200, 400, 800, and 1000 rpm, It was claimed that to keep carbon dioxide in solution experiment pressure must be 1000 psi. All experiments conducted at room-temperature 23°C. According to this work, the dissolution rate of calcite showed a significant reduction when 1.5 vol% of cationic acrylamide copolymer, 2 vol% corrosion inhibitor or 12 g/L citric acid added to the HCl

acid system. Also, the addition of polymer was changed the acid/rock reaction regime for both calcite and dolomite from mass-transfer to surface reaction limited. Unlike polymer, citric acid, and corrosion inhibitors 10 vol.% of mutual solvent was found to raise the rate of reaction for both calcite and dolomite by 9% and 29%, respectively. The same authors investigated the effect of iron(III) and the nonionic surfactant, while iron (III) reflect an inhibiting effect on the reaction rate the nonionic surfactant showed insignificant effect.

(Nasr-El-Din and Al-Mohammed 2006) made a set of experiments to examine the effect of viscoelastic surfactant on reaction rate of HCl/calcite using the rotating desk instrument. Calcite disks with 0.65 in thickness and 1.5 in diameter were used in this work. Surfactant concentration varied between 0–7 wt.%, the disk rotational speed was ranged from 100 rpm up to 1000 rpm. The temperature and the concentration of corrosion inhibitor were in the range of 25–85°C, 0.3–0.9 wt.% respectively. Experiments were conducted at 1000 psi with a fixed reaction time of 20 minutes and 20 wt.% HCl with different blends of surfactant and corrosion inhibitor concentration. The results of this study pointed out that the reaction rate of calcite is remarkably reduced by using the viscoelastic surfactant. Also, the dissolution rate was proved to be mass transfer limited.

(Khalid, Sultan, and Qiu 2015) evaluated the HCl diffusion coefficients effects on its reaction with calcite. Both coreflood and rotating disk apparatus experiments was used at reservoir condition to understand the impact of CO_2 on the reaction kinetics at this condition. A calcite disk of 1.5-inch diameter and 0.3-inch thickness was used in the reaction rate measurement part with RDA. These RDA experiments were conducted using 15wt % HCl, pressure range was from 1000 up to 3000 psi and disk rotational speed from (250–1250rpm) with a reaction temperature of 65°C.The second part of this work was

coreflood. Two cores of 12-inch length and 1.5-inch diameter were connected together in series to make the total effective length of the core 24-inch. Acid injected at a constant rate at the face of core 1 and then into core 2 in series. Pressure differential through cores was monitored and recorded while the outlet pressure kept constant at either 1000 psi or 3000 psi. This study concluded that at 3000 psi CO_2 will be in solution and that buffer hydrogen ions and slow down the reaction, therefore there is 50% reduction in the diffusion coefficient at 3000 psi compared to that at 1000 psi.

The coreflood experiments indicated that the pore volumes to break through PVBT for low injection rates at 1000 psi are in the range of 4–5 times that at 3000 psi while at a higher rate there was 25% difference. CT scan in revealed that at 1000 psi the produced wormholes volumes are doubled those at 3000 psi at low injection rate 2 cc/minor less, while at elevated rate 5cc/minthe effect of pressure on wormhole diameter is insignificant.

(Qiu et al. 2015) claimed that the diffusion coefficient (D_e) obtained at or below1000 psi is too low to simulate the reservoir conditions, and the D_e values from experiments based on fresh acid that has been neglecting the effect of reaction products and mainly CO_2 cannot represent real reaction kinetics of HCl/carbonate during acidizing treatment. So, a modified RDA has been used to generate the true reaction kinetics of spent acids at downhole conditions and accurate value of D_e for HCl/calcite, HCl/dolomite reaction rate. Experiments conducted at 1000 and 3000 psi at disk rotational speed from 250 –1250 rpm and a reaction temperature of 65°C. In the first set of experiment 15 wt.% HCl was used whereas at the second set 12.5, 10 & 7.5wt.% HCl used. The results of experiments indicate that D_e of HCl at high pressures is much lower than that at low pressure at same acid

concentration and this because of the impact of CO_2 brought out from the reaction of HCl-carbonate.

2.2 Reaction Kinetics of HCl with Dolomite

(K. C. Taylor, Mehta, and Aramco 2006) measured the reaction rates for reservoir rock from Saudi Arabia deep dolomitic gas reservoir in (275°F, 7500 psi).They used temperatures range of 23-85°C with 1 M HCl concentration at a disk rotational speed up to 800 rpm was studied. The main goal of the work was to study the effect of mineralogy on reservoir rock reaction kinetics. Eight distinct rock types that has wide-ranging in composition from 0%-100% dolomite were investigated. It was found that when the limestone reservoir rocks contain trace amount of clay impurities the acid dissolution rate was reduced by a factor of 25 which makes the acid reaction kinetics of these rocks similar to that of a fully dolomitized rock. Formation of a stable clay layer at the reacting surface of the rock work as a physical obstruction to acid reaction. Clays such as illite and mixed layer of illite/smectite decrease the reactionrates significantly. Rock samples containing 99% dolomite were more reactive due to the less amount of clay deposition on the surface of dolomite crystals. Moreover, it was also established that rock samples containing anhydrite interact with HCl solution created fine anhydrite needles that cause formation damage in tight carbonate reservoirs. In addition, the dissolution of anhydrite affected the calculation of dissolution rates leading to a reduction in acid reaction by 16%. On the other hand, preferential dissolution of calcite cause mechanical loss of dolomite crystals resulted in high dissolution rates as compared to the homogeneous rock of similar calcite and dolomite content.

(Khalid, Sultan, and Qiu 2015) investigated the impact of pressure on the reaction product of diffusion coefficient of HCl with dolomite. A modified RDA was used with 15wt.% fresh acid and different spent acid concentration of 12.5,10 and 7.5wt.%. Experiments conducted at 1000 and 3000 psi at disk rotational speed from 250–1250 rpm and a reaction temperature of 150°F, reacted acid samples were analyzed using Atomic Absorption Spectrometer (AAS). The experimental results concluded that D_e of HCl at high pressures is much lower than that at low pressure at same acid concentration and this because of the impact of CO_2 brought out from the reaction of HCl-dolomite. Moreover, a slight reduction of the diffusion coefficient occurred when the fresh acid was spent to 12.5 wt.%. In addition, at low disk rotational speed, the reaction was mass transfer limited whereas at high rotational speed the reaction was surface reaction limited. Also, rock porosity was found to have a significant effect on the diffusion coefficient since it affects the surface area of the reaction.

2.3 Reaction Kinetics of Gelled Acid with Calcite

Acids-soluble polymers are used in carbonate stimulation to reduce the reaction rate and acid leak-off by increasing its viscosity and provide a better acid diversion. (Nasr-El-Din et al. 2006) investigated the impact of these polymers on the reaction rate with calcite. Rotating disk instrument was used for reaction rate measurement which was done at 1000 psi, and temperature from 25–65°C and disk rotational speed from 100–1000 rpm whereas polymer concentration was varied between 0.5–2 wt.%. The results showed a remarkable increment in the apparent viscosity when polymer concentration increased from 0.5 to 1.5 wt.%. Also, it was found that there is a significant reduction in the reaction rate as the polymer concentration increased from 0.5 to 1.5 wt.%, whereas polymer increment to

2wt.% has a minor difference. Moreover, the calcite dissolution in gelled acid was found to be a function of RPM, temperature and polymer concentration.

(A I Rabie et al. 2010) studied the reaction rate kinetics and the mass transport of HCl in-situ gelled acid with carbonate rock. Different types of rock namely Edward limestone, Pink Dessert limestone, and Austin Chalk were prepared into 1.5-inch diameter and 1-inch length samples and their reaction with 5 wt.% in-situ gelled acid was measured using rotating disk apparatus. The dissolution rate measured at different temperature 150, 200, and 250°F, and disk rotational speed range of 100–1800 rpm. Experimental results indicated that mass transfer limited dissolution rate up to 1000 rpm while above 1000 rpm the reaction is surface reaction limited. On the other hand, diffusion coefficient, the reaction rate constant, and reaction activation energy at 150, 200, and 250 were reported. Moreover, the effect of crosslinker (Fe^{+3}) on the dissolution rate was studied and found to reduce the reaction rate by a factor of two compared with gelled acid at the same concentration of HCl.

2.4 Reaction Kinetics of Emulsified Chelating Agent with Calcite

(M. a Sayed et al. 2013), studied the reaction kinetics of an emulsified chelating agent (EGLDA) and limestone rock at a temperature of 230°F covering a disk rotational speed range from 100 to 1500 rpm. Moreover, the reaction rate of calcite in EGLDA was measured at temperatures of 250 & 300°F at 1000 rpm and these data were compared to the work done by (Ahmed I Rabie et al. 2011). It was concluded that emulsified GLDA achieved dissolution rates and diffusion coefficient that are less by two orders of magnitude as compared with emulsified acid at the same conditions.

2.5 Reaction Kinetics of Organic Acid with Calcite

(Al-douri et al. 2013) developed a new organic acid (phosphorus based and iron based) to stimulate deep wells in carbonate reservoirs. Reaction kinetics of the new organic acid was performed using rotating disk apparatus with calcite samples at 150, 200 and 250°F at variable disk rotational speeds (100-1500 rpm).

Firstly, reaction-rate experiments were conducted using the phosphorus based acid. It was found that the calcium concentration increased with the disk rotational speed at low temperatures. However, at high temperatures, the calcium concentration increased linearly for a certain period of time and then plateaued for the remainder of the reaction. The calcium concentration reached a maximum value of 2500 mg/l at 150°F and at 250°F whereas 4500 mg/l at 200°F. It was noted that the calcium concentration decreased when the temperature escalated from 200°F to 250°F due to the formation of phosphorus precipitate (calcium phosphate) on the core face.

2.6 Reaction Kinetics of Organic Acid with Dolomite

(Adenuga, Sayed, and Nasr-El-Din 2013) examined the reaction kinetics of dolomite rock sample with 0.866 N organic acids (acetic and formic acid) as well as Chelating Agents (GLDA) by varying the disk rotational speeds from 100 – 1500 rpm at 250°F. It was noted that as the disk rotational speed increased, magnesium concentration increased for all the acids. The dissolution rate was also determined using the plot of concentrations vs. reaction time and it was found that the reaction rate of GLDA solution was comparatively lower when compared to organic acids. It was also established that rate of dissolution of dolomite in GLDA was surface reaction limited at lower rotational speed values. However, at higher rotational speed, the reaction was mass transfer limited.

Acetic acid indicated variations as the rotational speed increased throughout the range. However, for formic acid, the reaction was mass transfer controlled until 1000 rpm. Diffusion coefficients were determined for organic acids and GLDA by plotting dissolution rate vs. square root of disk rotational speeds. The diffusion coefficient of GLDA was less as compared to organic acids. It was concluded that GLDA was more retarded than formic and acetic acid. Moreover, it is better suited for stimulation into a dolomitic reservoir than organic acids because their reaction rate was fast at high temperatures leading to inadequate acid penetration and wormhole creation into the formation.

2.7 Reaction Kinetics of Emulsified Acid with Calcite

(S. Al-Mutairi et al. 2009) studied in detail the effect of droplet size on the reaction kinetics of emulsified acids with calcite rocks. A set of experiments was conducted with different emulsified acids having three different emulsifier concentrations (1, 5 and 10 gpt) to investigate how the acid's droplet size would influence the reaction kinetics of acid with calcite. These experiments also were conducted at varying temperatures (25, 50 and 85°C) and disk rotational speeds (100 to 1000 RPM) using the Rotating Disk Apparatus.

Analysis of the calcitic disk's weight loss, the percentage of disk weight loss due to reaction with acid, with respect to emulsifier concentration showed that the weight loss increases when the emulsifier concentration was small. When emulsifier concentration increased, it produced a finer emulsion with smaller droplet size and more viscous. The viscosity of the emulsified acid has a role to restrict the movement of acid droplets from solution to rock surface and slow the reaction. In addition, analysis of calcium ion concentration in samples taken from the reaction vessel in the RDA showed that at an emulsifier concentration of 10 gpt the calcium concentration was smaller due to the smaller dissolution rate of rock disk.

(M. A. Sayed et al. 2012) presented a study in which an emulsified acid was developed to stimulate deep carbonate formation where high temperature has a significant impact on stability and reactivity of the acid-in-diesel emulsion system. The study involved coreflood experiments to investigate the effectiveness of acid emulsion in creating the wormholes. For that, they measured pressure drop across the core and calcium concentration, obtained from samples of core flood effluent fluids, as well as pH and density for different injection rates. For experimental work, they used two types of Indiana limestone cores, high-permeability cores, and low-permeability cores, in addition to five different injection rates (0.5, 1, 2, 5 and 10 cc/min) at a temperature of 300° F. From several coreflood runs, they were able to determine the optimum injection rate for low-permeability cores, 5 cc/min. At the optimum injection rate, the volume of acid required to achieve the breakthrough is minimum in compared to other injection rates. For the high-permeability limestone cores, there was no optimum rate of acid injection because the volume of acid injected was decreasing as the injection rate increased. However, they recommended using high injection rate when dealing with the high-permeability formation.

The reaction kinetics between acid and limestone rock was studied using the rotational disk apparatus. Several experiments were performed for emulsions with different emulsifier concentrations (0.5, 1 and 2 vol. %) and rotational speed up to 1500 rpm at 230° F. It was observed that the reaction rate of acid with limestone decreased when the emulsifier concentration increased. In addition, the dissolution rate increased when the rotational speed increased. This observation indicated that the reaction was mass-transfer limited. Slowest step in the reaction kinetics was the diffusion of acid droplets and reaction products between the acid solution and rock surface.

2.8 Reaction Kinetics of Emulsified Acid with Dolomite

(Kasza et al. 2006) presented a study on emulsified acid reactivity and compared it to that of straight HCl. Due to its weak performance, the hydrochloric and acetic acid solution had been used in BMB field in Poland before it was replaced by emulsified acid in acid matrix treatment. The high temperature in the formation caused the solution to react rapidly with the rocks; hence, the outcome of stimulation was not good. Laboratory tests revealed that the emulsified acid is the best solution for acidizing operation in that field. The measurements from the rotating disk apparatus showed that the reaction of the emulsified acid with carbonate formation was slower than that of plain HCl.

(M. A. Sayed and Nasrabadi 2013) used the Rotating Disk Machine to evaluate the reaction of the emulsified acid with dolomite. They tested several emulsions containing 15 wt.% HCl with different emulsifier concentrations (0.5, 1 & 2 vol.%) and various disk rotational speeds from 100 up to 1500 rev/min. Testing temperature condition was set at 230°F. Samples were taken from reactor vessel every one minute for a period of 10 minutes because of the high temperature. Magnesium and Calcium concentrations were measured and found to be increasing with time. At each emulsifier concentration, the dissolution rate was proportional to the disk rotational speed. Increasing disk rotational speed makes the acid droplets move faster which results in higher rate of reaction. Furthermore, it was noticed from their experiments that the diffusion coefficient decreased with increasing the emulsifier concentration. More amount of emulsifier in emulsion increases its viscosity, which, in turn, impedes the movement of acid droplets and makes the reaction rate slower. They also showed that the dissolution rate of dolomite rocks was lower than that of calcite

Table 2. 1 Reaction kinetics literature review summary 1

Paper	Authors	Parameter	Rock Type	Conditions	Fluid Type	Remarks
SPE 112454	Al-Mutairi et al 2008	1. Temperature (25, 50, 85 °C) 2. RPM (100 -1500) 3. Emulsifier concentration (1, 5, 10 gpt)	Calcite (1.5" diameter and 0.23" length)	1000 psi	Emulsified Acid (diesel + cationic emulsifier + corrosion inhibitor+Acid solution) (70: 30 acid to diesel ratio)	RDA D_e Calculation No Coreflood
SPE 133501	Rabie et al 2010	1. Temperature 150, 200, 250°F 2. RPM (100-1800) 3. Cross-linked Polymer conc. (.5, 1, 1.5, 2 wt.%)	Calcite (1.5" diameter and 1" length)	1500 psi	Regular Acid (5 wt.% HCL+CI) Gelled Acid (5 wt.% HCl+ polymer+CI) In-situ gelled acid(5 wt.%.HCL+Fe^{+3}+ CI + breaker, buffer)	RDA D_e calculation No Coreflood
SPE 151061	Sayed et al 2012	1. HCl concentration (5-8wt %) 2. RPM (100 up 1500) 3. Emulsifier concentration (.5, 1 and 2 vol %)	Calcite (N/A)	230 °F 1100 psi	Emulsified Acid (diesel + cationic emulsifier + corrosion inhibitor+Acid solution) (70: 30 acid to diesel ratio)	RDA Coreflood D_e Calculation
SPE 165120	Sayed et al 2013	1. Temperature 230, 250,300 F 2. RPM (100 up 1500) 3. Emulsifier concentration (.5, 1 and 2 vol %)	Indiana Lime Stone (Calcite) (1.5" diameter and 0.75" length)	N/A	Emulsified Chelating Agent (GLDT 20 wt.% + cationic emulsifier+diesel) (70: 30 acid to diesel ratio)	RDA Coreflood D_e Calculation
SPE 151815	Sayed et al 2013	1. RPM (100 up 1500) 2. Emulsifier concentration (.5, 1 and 2 vol %)	Dolomite (1.5" diameter and 0.75" length)	230 °F 1100 psi	Emulsified Acids (diesel + cationic emulsifier + corrosion inhibitor+ Acid solution) (70: 30 acid to diesel ratio)	RDA D_e calculation No coreflood
SPE 178967	Amy et al 2016	1. Fluid types (A, B, and C) 2. Flow rate (1, 2 and 5 cc/min)	Indiana Lime Stone 1.5" and 12'	300°F 3000 psi	Emulsified Acid (A, B, and C)	Coreflood No RDA

Table 2. 2 Reaction kinetics literature review summary 2

Reference	Authors	Parameter	Rock Type	Conditions	Fluid Type	Remarks
SPE 164110	Al-Douri et al. 2013	1. Temperature 150, 200, 250°F 2. RPM (100 up 1500) 3. Emulsifier concentration (.5, 1 and 2 vol %.)	Calcite (1.5" diameter and 0.75" length)	1500 psig	Organic Acid (phosphorus and iron based)	RDA Coreflood No D_e Calculation
SPE 165120	Saied et al 2013	1. Temperature 230, 250,300 F 2. RPM (100 up 1500) 3. Emulsifier concentration (.5, 1 and 2 vol %)	Indiana Lime Stone (Calcite) (1.5" diameter and 0.75" length)	N/A	Emulsified Chelating Agent (GLDT 20 wt.% + cationic emulsifier+diesel) (70: 30 acid to diesel ratio)	RDA Coreflood D_e Calculation
PETC 102838	Qui et al 2014	1. RPM (250 -1250) 2. Pressure (1000-3000) 3. Spent Acid concentration (12.5, 10, 7.5wt %)	Calcite (1.5" diameter,0.3" thickness)	65 °C	15 wt.% HCl	RDA Coreflood D_e Calculation
SPE 175832	Mohammad Ali et al 2015	1. RPM (250 -1250) 2. Pressure (1000-3000) 3. Spent Acid concentration (12.5, 10, 7.5wt %)	Dolomite (1.5" diameter and 0.27" length)	65 °C	15 wt.% HCl	RDA D_e calculation No Coreflood
SPE 174241	Qui et al 2015	1. RPM (250 -1250) 2. Pressure (1000-3000) 3. Spent Acid concentration (12.5, 10, 7.5wt %)	Dolomite & Calcite (N/A)	65°C	15wt.% HCl	RDA D_e Calculation No Coreflood

Table 2. 3 Reaction kinetics literature review summary 3

Reference	Authors	Parameter	Rock Type	Conditions	Fluid Type	Remarks
SPE 164110	Al-Douri et al 2013	1. Temperature 150, 200, 250°F 2. RPM (100 up 1500) 3. Emulsifier concentration (.5, 1 and 2 vol %)	Calcite (1.5" diameter and 0.75" length)	1500 psig	Organic Acid (phosphorus and iron based)	RDA Coreflood No D_e Calculation
SPE 164480	Adenuga et al 2013	1. RPM (100-1500) 2. Acid type(Acetic, Formic,GLDA)	Dolomite (1.5" diameter and 0.7" length)	250 °F 800+ psi	Simple organic acids (Acetic 5.2wt.%, Formic 3.6wt %) Chelating Agent (20 wt.% GLDA)	RDA D_e calculation No coreflood
PETC 102838	Qui et al 2014	1. RPM (250 -1250) 2. Pressure (1000-3000) 3. Spent Acid concentration (12.5, 10, 7.5wt %)	Calcite (1.5" diameter,0.3" thickness)	65 °C	15 wt.% HCl	RDA Coreflood D_e Calculation
SPE 175832	Mohammad Ali et al 2015	1. RPM (250 -1250) 2. Pressure (1000-3000) 3. Spent Acid concentration (12.5, 10, 7.5wt %)	Dolomite (1.5" diameter and 0.27" length)	65 °C	15 wt.% HCl	RDA D_e calculation No Coreflood
SPE 174241	Qui et al 2015	1. RPM (250 -1250) 2. Pressure (1000-3000) 3. Spent Acid concentration (12.5, 10, 7.5wt %)	Dolomite & Calcite (N/A)	65°C	15wt.% HCl	RDA D_e Calculation No Coreflood

CHAPTER 3

Research Methodology

In order to fulfill the objectives of this research several material and equipment were used. These materials and equipment were discussed in this chapter as well as the procedures for emulsified acid preparation, rotating desk experiments and Coreflood experiments setup.

3.1 Materials

3.1.1 Diesel

The diesel used in this study is commercial one provided from the local gas station. The surfactant is added to this diesel phase since it has the affinity to be mixed and distributed uniformly in it.

3.1.2 Waste Oil

Waste oil provided from a petrochemical industry and its composition is analyzed by (Sidaoui and Sultan 2016). Since any waste oil with different compositions will yield to unique emulsion characteristics (stability, rheology, and reactivity).

3.1.3 Hydraulic Acid

HCl 37 wt. % ACS grade was provided by a local company and produced by Sigma-Aldrich.

3.1.4 Emulsifier

A cationic emulsifier is supplied by the local service company. The emulsifier was used for preparing the diesel emulsified acid.

3.1.5 Nanoclays

Four types of Nano clays were used. Two of them showed good performance as an emulsifier. These Nano clays were provided from a BYK company.

3.1.6 Calcite Disks

From local outcrops, several carbonate blocks were obtained from an area near Central Saudi Arabia, Riyadh. Cores were drilled locally from these block then full screening was done. Screening based on porosity, permeability, and mineralogy. Only cores with 98% calcite and porosity less than 6% were used to make the smaller desk for RDA experiment. The disks dimension was the 1.5″ diameter and 0.75″ thickness. For each core sample porosity and permeability were measured and recorded.

3.1.7 Indiana Limestone Cores

Indiana limestone cores with average permeability range of 2–4 md and porosity of 15 % were drilled locally from one block supplied by Kocurek Industries, TX. The core sample with a 1.5″ diameter and 12″ length.

3.1.8 Crude Oil

Crude oil from the local field was used to saturate the disk for RDA experiments. The following table 3.1 is showing the Sara Analysis for this crude oil.

Table 3. 1 Sara analysis for the crude oil

Components (g)	Composition (%)
Saturated	26.64
Asphaltenes	6.90
Resin	5.54
Poly Aromatic Hydrocarbons	60.92
Total	100

3.2 Equipment

3.2.1 Rotating Disk Apparatus

The reaction kinetic experiments were done through the rotating disk apparatus RDA. This equipment is used to measure acid reaction rates, activation energy and reaction order in for acidizing fluids with carbonate rock. The rotating disk apparatus used in this study was manufactured by High-tech engineering with maximum operating conditions of 650°F, 5500 psi, and 3000 rpm. The rotating disk instrument is illustrated in Fig. 3.1. The main components of the RDA include reservoir, reaction vessel, poster pump, automatic sampling system, pressure regulators, flow lines and valves, temperature and pressure displays and data acquisition system. All acid wetted surfaces such as the reaction vessel, acid reservoir i.e. and liquid flow lines were fabricated from Hastelloy which is an acid resistant alloy. All other parts of the apparatus were fabricated from stainless steel.

Figure 3. 1 Rotating disk apparatus

3.2.2 Dual Coreflood System

The Dual Coreflood System used for the acidizing experiments is a high-pressure high-temperature core flow test equipment that comprises a fluid delivery pump, four fluid accumulators and two core holders capable of holding 12-inch core each placed in an oven, effluent accumulators and back pressure pumps. Both schematic and digital image for the system is illustrated in Fig. 3.2. The main parts of this system illustrated in Fig. 3.2 are following:

1. Injection pump
2. Accumulator (DI and Acid)
3. Pressure tapping
4. Confining stress
5. Axial stress
6. Accumulators for effluent
7. Back pressure pump

3.2.3 ICP-OES

Inductively coupled plasma optical emission spectrometry (ICP-OES) is an analytical technique, used for the detection of trace metals. Calcium concentration in the effluent samples taken from RDA experiment was measured using ICP-OES. In this method, an aqueous solution holding the metals or cations that are to be analyzed is subjected into a high energy argon plasma. Those metals entering this high energy region will be excited and then the spectral emissions that result are measured using a spectrometer set to a series of wavelengths specific to the elements being deticted. ICP-OES model Optima 8000 manufactured by PerkinElmer that used in this work is shown in Fig. 3.3. The functional

ranges for this system are down to the tens of ppb (µg/L) and up to the hundreds of ppm (mg/L).

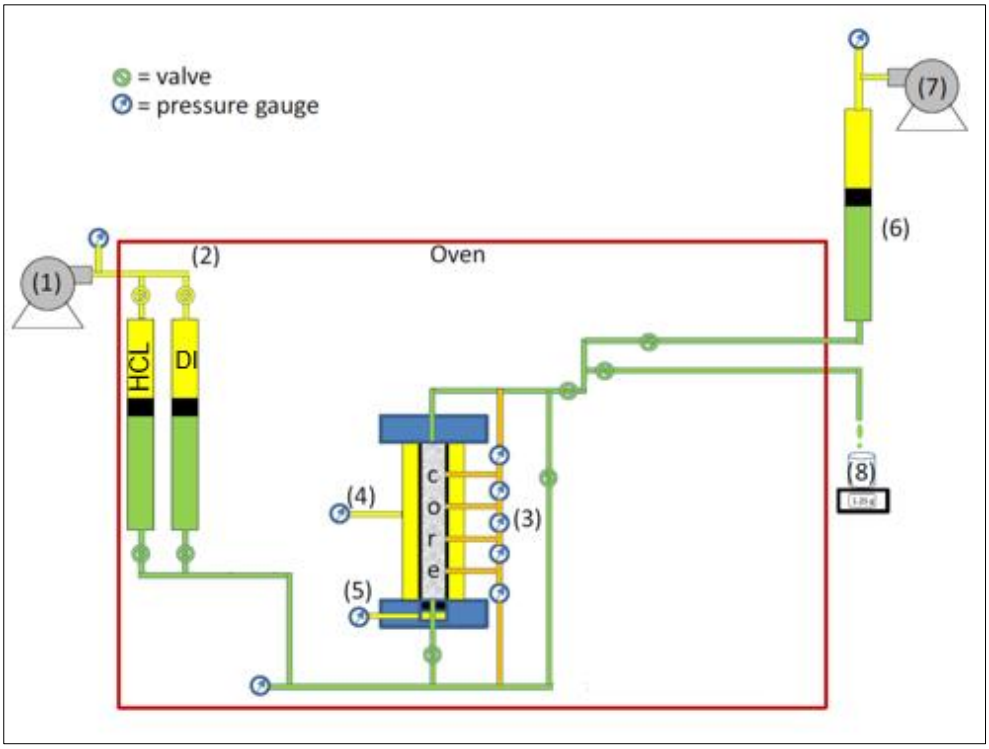

Figure 3. 2Dual core flood system

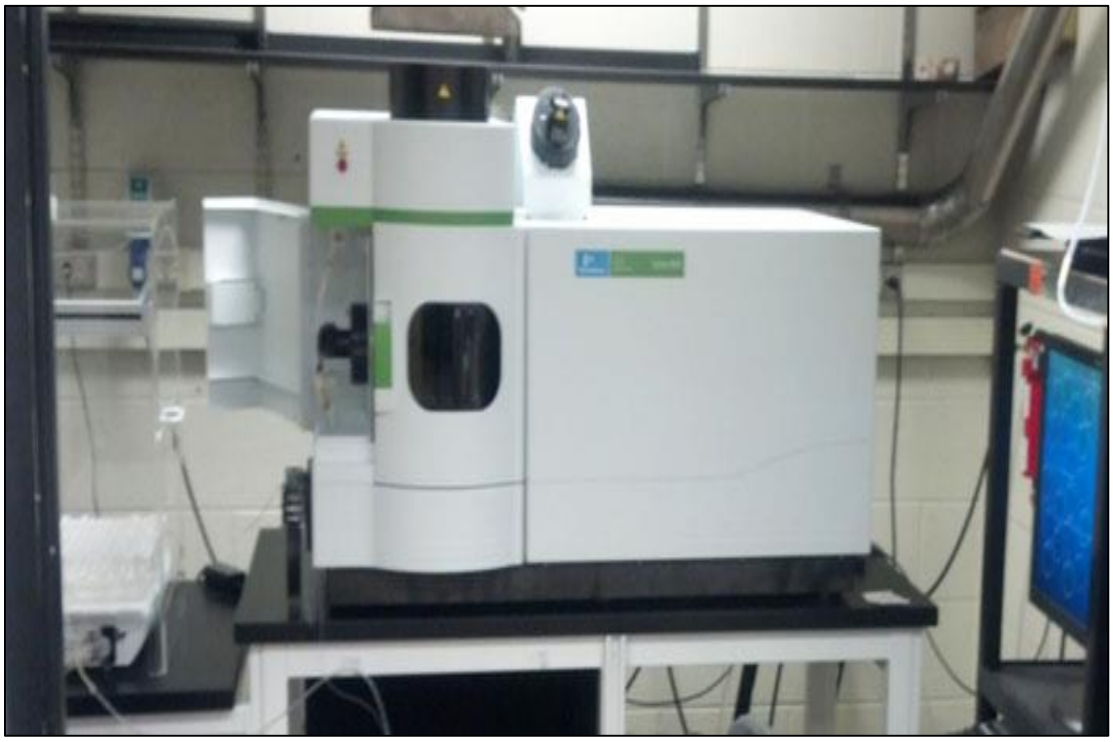

Figure 3. 3 ICP-OES

3.2.4 Toshiba Medical CT-Scanner Machine

Ct scans images were taken before the wormhole was created as well as after experiments using Toshiba Alexion TSX-032A medical X-ray CT scanner (resolution > 1 mm). This machine is illustrated in Fig. 3.4.

3.2.5 High Shear Mixer

The mixer illustrated in Fig. 3.5 was used in this study. It has a wide range of mixing speed (600–10,000) rpm. The device can be used to mix a volume of fluid from 0.25–30 liters. Also, it is equipped with an acid-resistant shaft so it can be used to prepare emulsified acid. This mixer model is T 50 manual ULTRA-TURRAX® from IKA®.

3.2.6 Dosimeter

Dosimat in Fig. 3.6 was used in emulsion preparation to add the acid phase at a constant rate into the diesel phase.

3.2.7 Conductivity Meter

The emulsion conductivity after each batch prepared and before the RDA and Coreflood experiment was measured using conductivity meter for quality check. The conductivity measurement was done through Mett0ler Toledo S3-Meter Seven2Go Portable Conductivity Meter shown in Fig. 3.7 with conductivity range of 0.010 µS/cm - 500 mS/cm. Also, this instrument has a conductivity resolution and accuracy of 0.001 and ±0.5% respectively.

Figure 3. 4 Toshiba CT scan machine

Figure 3. 5 High shear mixer

Figure 3. 6 Dosimat

Figure 3. 7 Conductivity meter

3.2.8 Oven

See through oven was used for emulsion stability detection as well as drying the disk before weight measurement.

3.2.9 Helium Porosimeter

Disks porosity and permeability were measured using Helium Porosimeter model AP-608 Automated Permeameter Porosimeter manufactured by Coretest System, INC, Fig 3.7. This machine has the capability to measure in a permeability range from 0.001 md up to10 d and the porosity range: 0.1% –40%.

3.2.10 Weighing Balance

A high accuracy weight balance was used for weight measurement of the calcite disks before and after the experiment as well as nanoclays for waste oil emulsified acid preparation. The weighing balance used in this study manufactured by Sartorius Company with 0.0001g resolution.

3.2.11 X-ray Diffraction

The mineralogy of the calcite disks used in reaction kinetics experiment with RDA was investigated using XRD analysis. The X-Ray Diffraction (XRD) machine used in disk analysis was from Rigaku company model Ultima IV shown in Fig 3.9.

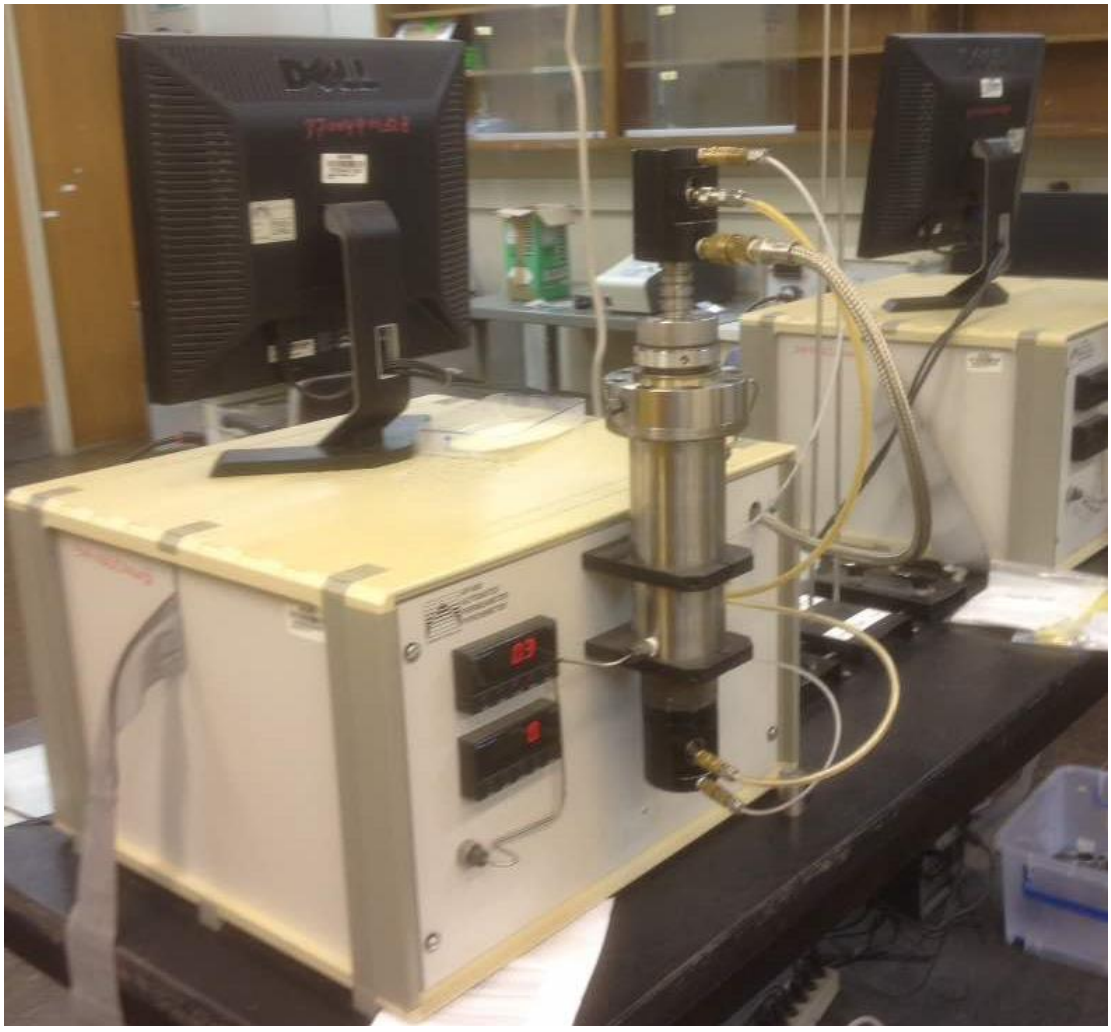

Figure 3. 8 Helium Porosimeter

Figure 3. 9 XRD equipment

3.3 Methodology

3.3.1 Diesel Emulsified Acid preparation

The diesel emulsified acid used for this set of experiment was prepared in a systematic manner so that the result will be reproducible.

- Firstly, a concentrated HCl 37wt. % was diluted to 28 wt. %. Using DI water.
- Corrosion inhibitor was added to the acid phase and mixed for 5 minutes using high speed mixed at 2000 rpm,
- Emulsifier was added the diesel phase and mixed as same as the acid phase
- Then acid was placed in dosimeter so it could be added at a constant rate (9 ml/min) to the diesel phase while mixing it at 2000 rpm with high shear mixer.
- Emulsion was blended for extra 2 minutes after the last acid drop so we can have a homogenous emulsion
- Finally, the prepared emulsion was tested to see whether the continuous phase is water or oil using both snake test and conductivity
- In the snake test, emulsion was injected into a beaker of water continuously. If the shape of the injected emulsion just like a snake and do not diffuse in the water phase, then we have a good emulsion. The second test was measuring emulsion conductivity, if it is zero or close to it then we have a good emulsion.
- Diesel with low sulfur and water content with known physical and chemical properties was used. Also, Emulsifier and corrosion inhibitor with 1 vol.% and 0.3 vol. % respectively were added to form the emulsion. Several type of surfactant was used and the one with highest stability at 135°C was chosen to formulate the emulsified acid for RDA and core-flow experiments.

Total 550 ml emulsion was prepared for each reaction kinetic experiment using rotating disk apparatus. Diesel and emulsifier (1 vol. % from total) volume were 165 ml while CI (0.3 vol. % from total) and acid volume was 385ml.The final Acid to diesel ratio was 70:30 by volume.

3.3.2 Waste oil emulsified acid preparation

Waste oil emulsified acid was prepared with waste oil to acid ratio of 70:30.

- Firstly, bactericide was added to waste oil with 10000 ppm concentration to the waste oil to reduce its odor.
- Then digital magnetic heater was used to stir and cook the mix at 75°C for 45 minutes to reduce the odor of the waste oil.
- Waste oil was filtered
- Nanoparticles were added to waste oil in 3000 ppm concentration and mixed for 30 minutes with a magnetic stirrer to form the oil phase.
- HCl with 28 wt. % was added to the oil phase at a rate of 6 ml/min using Dosimat.
- High shear mixer IKA® T 50 ULTRA-TURRAX was used while acid is being added to waste oil at 2000 RPM.
- After the last acid drop was added to the oil phase the mixing was continued for additional 15 minutes.
- Finally, conductivity, snake test and stability test for the emulsion were done to ensure that we good emulsion before RDA and Coreflood experiment.

3.3.3 Rotating disk experiment setup and procedures

The rotating disk apparatus was used to measure the reaction rate. The following procedure was followed for each experiment.

- The calcite disk was mounted on the rotating shaft using heat-shrink Teflon tubing. The shrinkage-tubing allows only the lower face of the disk to be exposed to HCl acid for reaction.
- Then prepared emulsified acid was transferred to the reservoir vessel.
- 300-400 psi is applied into the reservoir for transferring the fluid from the reservoir to the reactor and to prevent the expansion of emulsion when heat is applied.
- The reactor is heated to the desired temperature 135 °C and left until the temperature stabilized.
- The emulsified acid is also heated to 135 °C before transferring to the reactor.
- When both reactor and reservoir temperatures stabilized at 135°C the disk-rotational speed is turned on at the desired RPM.
- Then the fluid is transferred to the reactor and the timer switched on, after that the pressure is increased gradually to 3000psi.
- Samples were taken at each two minutes from the automatic sampling system for 20 minutes' reaction time.
- The sample then left to separate for one day and the 1ml from the aqueous phase was taken and diluted for ICP analysis to detect the calcium concentration with time.
- Then the reaction rate and diffusion coefficient were calculated.

3.3.4 Core-Flood Experiment Setup and Procedures

- CT-scanned Indiana limestone cores were placed in the high-temperature high-pressure HPHT Coreflood system described earlier.
- A confining pressure of approximately 1,500 psi more than the expected injection pressure was applied to both the cores.
- The core was then heated up to the desired temperature of 135°C.
- Before injecting the acid into the core, de-ionized water was injected to established stabilized flow in the cores at the desired back pressure i.e. 3000 psi.
- The pressure data from the outlet and inlet of cores at this point was used for the calculation of the initial permeability of the cores.
- After stabilization, acid was injected from one face of the core (inlet) which created wormholes in the core till they broke through from the other end (outlet).

3.4 Rotating Disk Theory

Rotating disk apparatus (RDA) is used widely to study diffusion coefficients, reaction order, dissolution rates, and activation energy of the reservoir rocks (K. Taylor, Al-Ghamdi, and Nasr-El-Din 2003). In heterogeneous reaction rate measurements, rates due to chemical reaction processes are differentiated from rates attributed to mass transfer processes. A rotating disk apparatus provides an opportunity to compare rates due to transport processes from rates as a result of chemical processes. Using the theory of mass transfer to rotating disk, it is possible to appraise the amount of diffusional resistance in the rotating disk system (Adenuga, Sayed, and Nasr-El-Din 2013)

For the rotating disk theory to be valid, certain experimental considerations need to be satisfied. The theory is invalidated as a result of a change in the evolution of the gaseous

reaction product CO2 at the solid liquid interface. In addition, the theory of rotating disk will remain valid for a system with finite geometry though it was derived assuming an infinite disk and fluid medium (Lund, Fogler, and McCune 1973)

In order to investigate the reaction of a fluid with a solid surface using RDA, the following condition must be confirmed (Adenuga 2013):

i. Flow in the vicinity of the disk must be laminar i.e. the Reynolds number must be in between 10^4 and 10^5.

ii. The disk is assumed to be an infinite plane; hence the disk diameter must be larger than the thickness of the diffusion layer boundary.

iii. The disk is assumed to be spinning in a fluid of infinite volume.

Newman (1965) pointed out that the rate of mass transfer, J_{mt}, for Newtonian fluids, to the rotating disk apparatus in laminar flow regime is given by:

$$J_{mt} = \frac{0.62048\ (S_c)^{-2/3}(v\omega)^{1/2}}{1 + .2980(S_c)^{-1/3} + .1451(S_c)^{-\frac{2}{3}}} \times (C_b - C_s)$$

Where:

J_{mt} = mass transfer rate of HCl to a rotating disk apparatus, mole/s. cm2

v = kinematic viscosity, cm^2/sec

ω = disk rotational speed, rad/sec

C_b = acid bulk concentration, moles/ cm^3

Cs = acid surface concentration, moles/ cm^3

Sc = Schmidt number = ν / D

D = diffusivity of HCl, cm^2/sec

Lund et al. (1973) described the rate of surface reaction dependency on concentration by the power law model expression that can be represented by:

$$-r_{HCL} = k\, C_s^n$$

Where

$-r_{HCL}$ = rate of reaction in moles/s.cm^2

k = reaction rate constant in (moles/cm^2.s) (mole/cm^3)$^{-n}$

n = reaction order, dimensionless

C_s = surface acid concentration in moles/cm^3

The detailed solution of the Navier-Stokes and continuity equation in the convective diffusion to the surface of the rotating disk for Newtonian fluids is shown below:

In the cylindrical coordinate system, the Navier-Stokes equation and continuity equations take the form:

$$\frac{V_\emptyset}{r}\frac{\partial V_r}{\partial r} + V_r\frac{\partial V_r}{\partial r} - \frac{V_\emptyset^2}{r} + V_y\frac{\partial V_r}{\partial y} = -\frac{1}{\rho}\frac{\partial P}{\partial r} + \nu\left(\Delta V_r - \frac{V_r}{r} - \frac{2}{r^2}\frac{\partial V_\emptyset}{\partial \emptyset}\right) \quad \text{..... (1)}$$

$$\frac{V_\emptyset}{r}\frac{\partial V_\emptyset}{\partial \emptyset} + V_r\frac{\partial V_\emptyset}{\partial r} + \frac{V_r V_\emptyset}{r} + V_y\frac{\partial V_\emptyset}{\partial y} = -\frac{1}{\rho r}\frac{\partial P}{\partial \emptyset} + \nu\left(\Delta V_\emptyset - \frac{V_\emptyset}{r^2} - \frac{2}{r^2}\frac{\partial V_r}{\partial \emptyset}\right) \quad \text{..... (2)}$$

$$\frac{V_\emptyset}{r}\frac{\partial V_y}{\partial \emptyset} + V_r\frac{\partial V_y}{\partial r} + V_y\frac{\partial V_y}{\partial y} = -\frac{1}{\rho}\frac{\partial P}{\partial y} + v(\Delta V_y) \quad \ldots\ldots\ldots\ldots\ldots\ldots\ldots\ldots (3)$$

$$\frac{1}{r}\frac{\partial V_\emptyset}{\partial \emptyset} + \frac{\partial V_r}{\partial r} + \frac{\partial V_y}{\partial y} + \frac{V_r}{r} = 0 \ldots\ldots\ldots\ldots\ldots\ldots\ldots\ldots (4)$$

At the surface of the disk the following boundary conditions must be satisfied:

$V_r = 0$, $V_\emptyset = \omega$, and $V_y = 0$ at $y = 0$……..(5)

In order to the fluid to be continuously supplied to the disk surface, an axial vertical flow must be maintained. Therefore, the boundary conditions at infinity are

$V_r = 0$, $V_\emptyset = 0$, and $V_y = U_0$ at $y \to \infty$……(6)

Because of the axial symmetry, all derivatives with respect to the angle ∅ vanish. Also, the pressure of the fluid may be considered constant along the radius r. Then, equations 1,2 and 3 might be written as follows:

$$V_r\frac{\partial V_r}{\partial r} - \frac{V_\emptyset^2}{r} + V_y\frac{\partial V_r}{\partial y} = v\left(\frac{\partial^2 V_r}{\partial y^2} + \frac{\partial^2 V_r}{\partial r^2} + \frac{1}{r}\frac{\partial V_r}{\partial r} - \frac{V_r}{r^2}\right) \quad \ldots\ldots\ldots\ldots\ldots\ldots\ldots\ldots (7)$$

$$V_r\frac{\partial V_\emptyset}{\partial r} + \frac{V_r V_\emptyset}{r} + V_y\frac{\partial V_\emptyset}{\partial y} = v\left(\frac{\partial^2 V_\emptyset}{\partial y^2} + \frac{\partial^2 V_\emptyset}{\partial r^2} + \frac{1}{r}\frac{\partial V_\emptyset}{\partial r} - \frac{V_\emptyset}{r^2}\right) \quad \ldots\ldots\ldots\ldots\ldots\ldots\ldots\ldots (8)$$

$$V_r\frac{\partial V_y}{\partial r} + V_y\frac{\partial V_y}{\partial y} = -\frac{1}{\rho}\frac{\partial P}{\partial y} + v\left(\frac{\partial^2 V_y}{\partial y^2} + \frac{\partial^2 V_y}{\partial r^2} + \frac{1}{r}\frac{\partial V_y}{\partial r}\right) \quad \ldots\ldots\ldots\ldots\ldots\ldots\ldots\ldots (9)$$

We search for a solution satisfy the continuity equation and the boundary conditions (equation 5 and 6) in the form

$$V_r = r\,\omega\,F(\xi)$$

$$V_{\emptyset} = r\ \omega\ G(\xi)$$

$$V_y = \sqrt{v\omega}\ H(\xi)$$

$$p = -\rho v\omega\ P(\xi)$$

Where the independent variable is the dimensionless quantity

$$\xi = \sqrt{\frac{\omega}{v}}\,\mathrm{y}$$

$$F^2 - G^2 + F'H = F'' \ldots\ldots\ldots\ldots\ldots\ldots\ldots\ldots\ldots\ldots\ (11)$$

$$2FG + G'H = G'' \ldots\ldots\ldots\ldots\ldots\ldots\ldots\ldots\ldots\ldots\ (12)$$

$$H'H = G'' + P' \ldots\ldots\ldots\ldots\ldots\ldots\ldots\ldots\ldots\ldots\ (13)$$

$$2F + H' = 0 \ldots\ldots\ldots\ldots\ldots\ldots\ldots\ldots\ldots\ldots\ (14)$$

And the boundary conditions:

$$F = 0, G = 1, F = 0, \xi = 0 \ldots\ldots\ldots\ldots\ldots\ldots\ldots\ldots\ (15)$$

$$F \to 0, G \to 1, F \to -\alpha, as\ \xi \to 0 \ldots\ldots\ldots\ldots\ldots\ldots\ldots\ldots\ (16)$$

All of which is obtained by substituting the definition of V_r, $V_{\emptyset}$ and V_y into the Navier-Stakes and continuity equations, and into the boundary conditions, The constant $\alpha = \frac{U_0}{\sqrt{v\omega}}$ is to be determined.

The functions F, G, and H may be made to satisfy the above equations and boundary conditions by formal series expansions. The nature of these expansions for large values of ξ (asymptotic expansion is suggested by the boundary conditions for H.

From this similarity solution, it was found

$$V_y \approx -0.89\sqrt{v\omega} \qquad as \quad y \to \infty \ldots\ldots (17)$$

$$V_y \approx -0.51\sqrt{\frac{\omega^3}{v}}\, y^2 \qquad for\ y \ll \sqrt{\frac{v}{\omega}} \ldots\ldots (18)$$

The boundary layer δ_0

$$\delta_0 = 3.6\sqrt{\frac{v}{\omega}} \ \ldots\ldots (19)$$

The Diffusion problem

The convective diffusion equation in cylindrical coordinates takes the form

$$V_r\frac{\partial c}{\partial r} + \frac{V_\emptyset}{r}\frac{\partial c}{\partial \emptyset} + Vy\frac{\partial c}{\partial y} = D\left(\frac{\partial^2 c}{\partial y^2} + \frac{\partial^2 c}{\partial r^2} + \frac{1}{r}\frac{\partial c}{\partial r} + \frac{1}{r^2}\frac{\partial^2 c}{\partial \emptyset^2}\right) \ldots\ldots (20)$$

The boundary conditions are

$$c = c_0 \qquad as \qquad y \to \infty \ldots\ldots (21)$$

Where c_0 is the concentration in the bulk of the solution. For a maximum diffusional flux, the following condition prevails at the disk surface

$$c = 0 \qquad at \qquad y = 0 \ldots\ldots (22)$$

We are looking for a solution for equation 20 that satisfy the boundary conditions (21) and (22) in the form

$$c = c(y); \ldots\ldots (23)$$

Assume the concentration is only a function of the distance from the surface of the disk and is not a function of either r or ∅.

Then equation (20) becomes

$$Vy\frac{\partial c}{\partial y} = D\frac{\partial^2 c}{\partial y^2} \quad \text{..... (24)}$$

By integrating equation (24), we get

$$\frac{\partial c}{\partial y} = a_1 \exp\left\{\frac{1}{D}\int_0^y V_y(z)dz\right\} \quad \text{..... (25)}$$

And by a second integration

$$c = a_1 \int_0^y \exp\left\{\frac{1}{D}\int_0^t V_y(z)dz\right\} dt + a_2 \quad \text{..... (26)}$$

The constants a_1 and a_2 are found from boundary conditions and the latter immediately yields

a_2=0

Since, at y=0, the integral in (26) becomes zero. Also, because of boundary condition (21)

$$c = a_1 \int_0^\infty \exp\left\{\frac{1}{D}\int_0^t V_y(z)dz\right\} dt \quad \text{..... (27)}$$

Now the integral will be divided into two parts from 0 to the boundary layer $\delta_0$and from the boundary layer δ_0 to infinity

$$c = \int_0^{\infty} \exp\left\{\frac{1}{D}\int_0^t V_y(z)dz\right\}dt$$

$$= \int_0^{\delta_0} \exp\left\{\frac{1}{D}\int_0^t V_y(z)dz\right\}dt + \int_{\delta_0}^{\infty} \exp\left\{\frac{1}{D}\int_0^t V_y(z)dz\right\}dt = J_1 + J_2$$

Using equation 18 and neglecting the higher order terms in the expansion of V_y we obtain for J_1

$$J_1 = \int_0^{\delta_0} exp\left\{-\frac{\omega^{3/2}t^3}{5.88Dv^{1/2}}\right\}dt$$

introducing new variable u

$$u = \frac{\omega^{1/2}t}{\sqrt[3]{5.88}\, D^{2/3}v^{1/6}} \ldots\ldots\ldots\ldots\ldots\ldots\ldots\ldots\ldots\ldots\ldots (27)$$

Then we find that

$$J_1 \approx \frac{\sqrt[3]{6}D^{1/3}v^{1/6}}{\omega^{1/2}}\int_0^{\frac{\delta_0\omega^{1/2}}{\sqrt[3]{6}D^{1/3}v^{1/6}}} e^{-u^3}du = \frac{1.81D^{1/3}v^{1/6}}{\omega^{1/2}}\int_0^{2\left(\frac{v}{D}\right)^{1/3}} e^{-u^3}du$$

For $\frac{v}{D} \gg 1$, the upper limit of the integral is significantly greater than unity, and, since the integrand decreases rapidly for values of the argument greater than unity, we can replace the upper limit by infinity. Then

$$J_1 \approx \frac{1.81D^{1/3}v^{1/6}}{\omega^{1/2}}\int_0^{\infty} e^{-u^3}du$$

Thus because of the rapid convergence of the integral for $v \gg D$ it is possible to use only the first term of expansion of $V_{y>}$

The integral of J_1 may be expressed by Γ function

$$\int_0^\infty e^{-u^3} du = \frac{1}{3}\int_0^\infty e^{-t} t^{-2/3} dt = \frac{1}{3}\Gamma\left(\frac{1}{3}\right) = \Gamma\left(1+\frac{1}{3}\right) = \Gamma\left(\frac{4}{3}\right) \approx 0.89$$

Therefore, finally

$$J_1 = \frac{1.61166\, D^{1/3} v^{1/6}}{\omega^{1/2}}$$

The integral J_2 is computed in a similar manner:

$$J_2 = \int_{\delta_0}^\infty \exp\left\{\frac{1}{D}\int_0^t V_y(z)dz\right\} dt = \int_{\delta_0}^\infty \exp\left\{-\frac{0.89\sqrt{v\omega}}{D} t\right\} dt$$

$$= \frac{D}{0.89\sqrt{v\omega}} exp\left\{-\frac{0.89\sqrt{v\omega}}{D}\delta_0\right\} = \frac{D}{0.89\sqrt{v\omega}} e^{-3\left(\frac{v}{D}\right)}$$

For $v \gg D$, the value of the integral J_2 is very smale compared to J_1 and can be omittted thus

$$J \approx J_1$$

And from (27) we find that

$$a_1 = \frac{c_0}{J_1}$$

Finally, for a concentration distribution that satisfied both the convective diffusion equation and the boundary conditions we obtain

$$c = \frac{c_0}{J_1}\int_0^y \exp\left\{\frac{1}{D}\int_0^t V_y(z)dz\right\}dt = \frac{c_0}{1.61\left(\frac{v}{D}\right)^{1/3}\sqrt{\frac{v}{\omega}}}\int_0^y \exp\left\{\frac{1}{D}\int_0^t V_y(z)dz\right\}dt \text{.....(28)}$$

In order to determine c as a function of distance y from the surface of the disk (where y=0) we substitute V_y in (28) by its definition from (18). Then the equation for the concentration distribution for $(y < \delta_0)$ can be written in a symmetrical form

$$c = c_0 \frac{\int_0^Y e^{-u^3}du}{\int_0^\infty e^{-u^3}du} \text{..... (29)}$$

Where u is defined, as before, by formula (27') and Y denotes the ratio

$$Y = y{:}\frac{\sqrt[3]{6}D^{2/3}}{\omega^{1/2}} \approx \frac{2y}{\delta_0}\left(\frac{v}{D}\right)^{1/3}$$

Differentiating (29) we obtain the mass flux to the disk surface

$$j = D\left(\frac{\partial c}{\partial y}\right)_{y=0} = \frac{Dc_0}{0.89}\frac{\omega^{1/2}}{\sqrt[3]{6}\,D^{1/3}v^{1/6}} = \frac{Dc_0}{1.61\left(\frac{v}{D}\right)^{1/3}\sqrt{\frac{v}{\omega}}} = 0.62\,D^{-2/3}v^{-1/6}\omega^{1/2}c_0 \text{..... (30)}$$

$$\boldsymbol{j = 0.62\,D^{-2/3}v^{-1/6}\omega^{1/2}c_0}$$

Emulsified acid was found to be non-Newtonian fluid following power-law model, the viscosity of these fluids can be given by

$$\mu_a = K\gamma^{n-1}$$

where,

K = power law consistency index, g/cm. $s^{(n-2)}$

n = power law index

μ_a = apparent fluid viscosity, cp

γ = shear rate, s^{-1}

(Hansford and Litt 1968) resolved the equation of convective diffusion and the Schmidt and Reynolds numbers were altered to take into account the dependency of shear rate on the power-law viscosity. The solution was finally presented in the form of three dimensionless numbers N_{Sh}, N_{Re}, N_{sh}.

The detailed solution of the Navier-Stokes and continuity equation in the convective diffusion toward the surface of the rotating disk for non-Newtonian fluids

Starting from Nervier-Stoke and continuity equation for the cylindrical coordinate system the solution is similar to that of the Newtonian fluid with some differences in transformation variable and the definition of Reynolds and Schmidt numbers. The solution was based on the definition of a dimensionless transformation variable that includes the power-law parameters.

$$\xi = z\left(\frac{\omega^{2-n} r^{1-n}}{N}\right)^{\frac{1}{1+n}} \quad \ldots\ldots\ldots\ldots\ldots\ldots\ldots\ldots\ldots\ldots (1)$$

Then dimensionless velocity coordinates defined below as functions of the transformation variable ξ:

$$u(r,z) = \omega r F(\xi) \ldots\ldots\ldots\ldots\ldots\ldots\ldots\ldots (2)$$

$$v(r,z) = \omega r G(\xi) \ldots\ldots\ldots\ldots\ldots\ldots\ldots\ldots (3)$$

$$\mathrm{w(r,z)} = [\mathrm{r}^{n-1}\ \omega^{2n-1}\mathrm{N}]^{\frac{1}{1+n}}\mathrm{H}(\xi) \ldots\ldots\ldots\ldots\ldots\ldots\ldots\ldots (4)$$

motion equations and continuity equation can then be transformed into ordinary differential equations in terms of F, G, and H. In this work, the continuity is only equation required:

$$2\mathrm{F} + \mathrm{H}' + \left(\frac{1-n}{1+n}\right)\mathrm{F}'\,\xi = 0 \ldots\ldots\ldots\ldots\ldots\ldots\ldots\ldots (5)$$

Now the transformation will be extended to the equation of convective diffusion, which in cylindrical coordinates for boundary layer flow is expressed as:

$$w\frac{\partial c}{\partial z} = D\frac{\partial^2 c}{\partial z^2}$$

$$c = c_0 \quad at \ \ z = 0$$

$$\mathrm{c} = 0 \quad \text{for } \mathrm{z} \to \infty \ldots\ldots\ldots\ldots\ldots\ldots\ldots (6)$$

Then we define the dimensionless concentration as:

$$C(\xi) = \frac{c(r,z)}{c_0} \quad \text{..... (7)}$$

And this will reduce the diffusion equation to

$$C'' = [N_{Re}]^{n-1/n+1} HC' N_{Sc} = N_{PL} HC'$$

$$C = 1 \quad \text{at} \quad \xi = 0$$

$$C = 0 \quad \text{at} \quad \xi \to 0 \text{.....(8)}$$

The Schmidt and Reynolds numbers are defined to involve the shear dependence of the power-law "viscosity:

$$N_{Re} = \frac{r^2 \omega^{2-n}}{N}; \quad N_{Sc} = \frac{N\omega^{(n-1)}}{D} \text{.....(9)}$$

Integrating equation 11

$$N_{PL} = \frac{1}{D}[r^{2(n-1)} \omega^{3(n-1)} N^2]^{1/1+n} \text{..... (10)}$$

the dimensionless radial velocity can be obtained by:

$$F = a\,\xi \text{..... (11)}$$

Defining $a = F'(0)$ which is the gradient of dimensionless radial velocity at the surface of the disk. Substitute the F value into the equation of continuity. Eq. (5).

$$2a\xi + H' + \left(\frac{1-n}{1+n}\right) a\xi = 0$$

$$H' = -2a\left[1 + \frac{1}{2}\left(\frac{1-n}{1+n}\right)\right]\xi = -2a'\xi \text{..... (12)}$$

Since H(0)= 0, when equation 12 integrated it will yield the following

$$H = -a'\xi^2 \text{.....(13)}$$

put this into equation. (5), we will have

$$C'' = -a' N_{PL} \xi^2 C' \text{..... (14)}$$

Then Integrate equation (14) two times with the assumed boundary conditions to give

$$C(x) = 1 - \frac{\Gamma\left(\frac{1}{3},x\right)}{\Gamma\left(\frac{1}{3},\infty\right)} \ldots\ldots\ldots\ldots\ldots\ldots\ldots\ldots\ldots\ldots \quad (15)$$

Where

$$x = \left(\frac{a'N_{PL}}{3}\right)\xi^3$$

at the surface of the disk the local mass flux is obtained by

$$j(r) = -D\left(\frac{\partial c}{\partial z}\right)_0 = -D\left[\frac{\omega^{2-n}r^{1-n}}{N}\right]^{1/1+n} C'(\xi)|_{\xi=0} \ldots\ldots\ldots\ldots\ldots\ldots\ldots\ldots\ldots\ldots \quad (16)$$

When differentiating equation 16, and convert to the ξ system, we will have

$$C'(\xi)|_{\xi=0} = \left[\frac{a'N_{PL}}{3}\right]^{1/3} \Big/ \frac{1}{3}\Gamma\left(\frac{1}{3}\right)$$

In this case the $\Gamma(n)$ is the gamma function and the mass flux will be

$$j(r) = \frac{c_0}{\frac{1}{3}\Gamma\left(\frac{1}{3}\right)}\left[\frac{\omega^{2-n}r^{1-n}}{N}\right]^{1/1+n}\left[\frac{a'N_{PL}}{3}\right]^{1/3} \ldots\ldots\ldots\ldots\ldots\ldots\ldots\ldots \quad (17)$$

and replacing for N_{PL} from equation 10, and merging terms, we have

$$j(r) = \left(\frac{a'}{3}\right)^{1/3}\left[\frac{C_0 D^{\frac{2}{3}}}{\frac{1}{3}\Gamma\left(\frac{1}{3}\right)}\right][N]^{-1/3(1/1+n)}[r]^{1/3(1-n/1+n)}[\omega]^{1/1+n} \ldots\ldots\ldots\ldots\ldots\ldots\ldots\ldots (18)$$

Integrating the local flux across the surface of the disk the average mass flux is given as:

$$J(R) = \left(\frac{a'}{3}\right)^{1/3}\left[\frac{1}{\frac{1}{3}\Gamma\left(\frac{1}{3}\right)}\right]\left[\frac{6n+6}{5n+7}\right]C_0 D^{\frac{2}{3}}[N]^{-1/3(1/1+n)}[R]^{1/3(1-n/1+n)}[\omega]^{1/1+n} \ldots (19)$$

overall Sherwood number could by defined by

$$N_{Sh} = \frac{kR}{D} = \frac{JR}{C_0 D} \ldots\ldots\ldots\ldots\ldots\ldots\ldots\ldots\ldots\ldots\ldots\ldots\ldots\ldots\ldots\ldots\ldots\ldots\ldots\ldots\ldots\ldots (20)$$

and lastly become

$$N_{Sh}(R) = \left(\frac{1}{0.89}\right)\emptyset(n)N_{Sc}^{1/3}N_{Re}^{1/3(n+2/n+1)} \ldots\ldots\ldots\ldots\ldots\ldots\ldots\ldots\ldots\ldots\ldots\ldots\ldots\ldots\ldots\ldots\ldots\ldots\ldots\ldots\ldots\ldots (21)$$

Where

$$\frac{1}{3}\Gamma\left(\frac{1}{3}\right) = 0.89$$

$$\emptyset(n) = \left(\frac{6n+6}{5n+7}\right)\left(\frac{a\prime}{3}\right)^{1/3} \ldots\ldots\ldots\ldots\ldots\ldots\ldots\ldots\ldots (22)$$

Substituting the values of N_{Sh}, N_{Re}, N_{sh} in equation (21) and solve for average flux we got the following

$$\boldsymbol{J = \left[\emptyset(n)\left(\frac{K}{\rho}\right)^{-1/(3(n+1))} r^{(1-n)/3(n+1)}\omega^{1/(1+n)}D^{2/3}\right]c_0 = A\omega^{1/(1+n)}} \ldots\ldots\ldots\ldots\ldots\ldots (23)$$

NOTATION

a Constant in

a' constant defined by equation (15)

c concentration, gcmW3

c_0 solubility, gcmm3

C dimensionless concentration defined by equation. (l0)

D diffusivity, cm^2/sec

F, G, H dimensionless radial, tangential and axial velocities defined in Eq. (8)

j local mass flux, gcm-2sec^{-1}

J average mass flux, g /sec-cm^2

K power-law consistency index, g /sec-cm^2

n power-law behavior index

N K/ρ, cm^2sec-'nf2'

N_{Re} Reynolds number

N_{Sh} Sherwood number

N_{Sc} Schmidt number

N_{PL} dimensionless group described by equation 13

r radial coordinate, cm

R radius, cm

CHAPTER 4

Core Flood Experiments Results

4.1 Core Flood Study

In this part of the study, a series of 8 Coreflood experiments were done using Indiana limestone cores. The objectives of the first 4 experiments were to study the performance of the new waste oil emulsified acid and its reactivity with calcite at high pressure and high-temperature HPHT conditions where the emulsified acid is recommended for field application. While the second set of the 4 experiment was used for comparison with conventional diesel emulsified acid at same pressure and temperature. For all the experiments, firstly, the desired temperature of 135°C was achieved and stabilized and then DI water was injected into the core at the specific flow rate for each experiment while maintaining the back pressure applied at the outlet at 3000 psi. The stabilized flow was identified by the stable values of pressure at the inlet and outlet of the core for both pressure transducers that used to calculate the pressure drop during injection. The permeability of the cores was determined from the pressure data points taken from these transducers after flow stabilized. The acid is then injected into the core and as it touches the face of the core and begins to dissolve the carbonate rock, a wormhole is generated and indicated by the pressure drop in the first section. While the wormhole propagates along the length of the core, the pressure differential across the core keeps on coming down to zero and that

is when a breakthrough occurs. The volume of emulsified acid consumed by the core is called the breakthrough volume and is calculated in terms of pore volumes of emulsified acid injected to breakthrough.

Table 4. 1 Core flood experiment schedule

28 wt. % HCl Indiana Limestone core 12" length and 1.5" Diameter Temperature 135 °C and 3000 psi		
Acid type	Run #	Injection rate cc/min
Diesel Emulsified Acid	1	0.5
	2	2
	3	5
	4	10
Waste oil Emulsified Acid	5	0.5
	6	2
	7	5
	8	10

4.2 Basic Analysis description

The data logs for all the experiments include logging time, valve configuration, pressure values at the pumps, confining and triaxial pressures, inlets, outlets, pressure tappings, temperature values at various points etc. From the valve configuration and the notes taken during the experiments, the time of injection of acid is determined. Pressure differentials in specific sections are plotted against time of acid injection which shows a sharp drop to zero indicating the propagation of wormhole Through them. This breakthrough time is visually determined and used for all subsequent calculations. The following definitions give a description of the terms used for the basic analysis of all the Core flood experiments.

Time to Breakthrough (hours): It is the time at which emulsified acid breakthrough the core to reach its outlet. Its values are manually entered by observing the pressure drop

charts. For the dual core flood system that we used the breakthrough, criteria are achieved when the pressure drops a cross the core is 10 psi.

Total Emulsified Acid Volume Injected: Since the injection rate is constant, the total Breakthrough volume is calculated by the following formula:

$$Total\ Emulsified\ acid\ injected = Injection\ rate * breakthrough\ time$$

Dead volume: This is the volume of the line from the accumulator to the core inlet and it is found to be 5 cm3.

Actual Volume to Breakthrough (AVBT) (cm3): Actual Breakthrough Volume is calculated by subtracting the dead volumes from the Apparent Breakthrough Volume.

Pore Volume to Breakthrough (PVTB): The Actual Volume to Breakthrough is converted in terms of Pore volumes by dividing this volume by the total pore volumes of the core.

4.3 Stability of Emulsified Acids at 135°C.

Emulsified acid should be stable during the whole injection time. The waste oil emulsified acid was stable for more than four hours. while diesel emulsified used in this study showed 11 hours' stability at 135°C.The thermal stability for both waste oil and diesel emulsified acids used in coreflood experiments is shown Fig. 4.1 and Fig. 4.2**.**

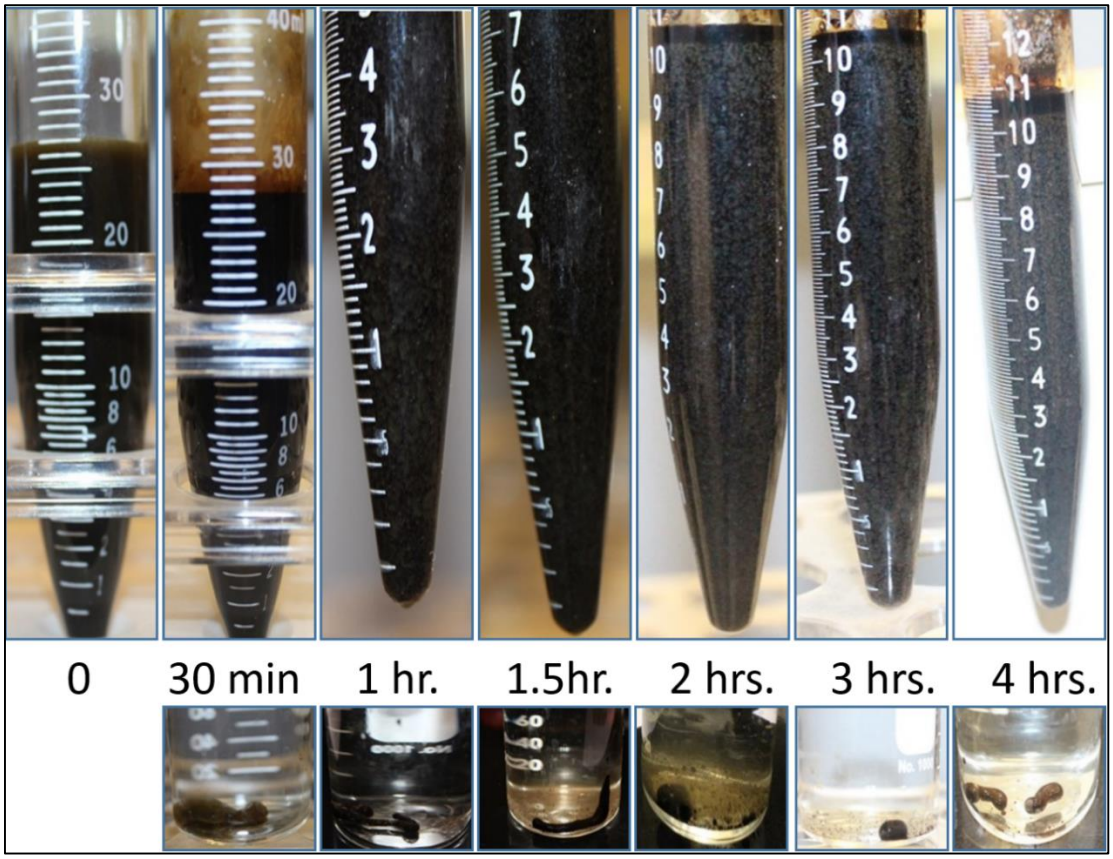

Figure 4. 1 Waste oil emulsified acid stability at 135°C

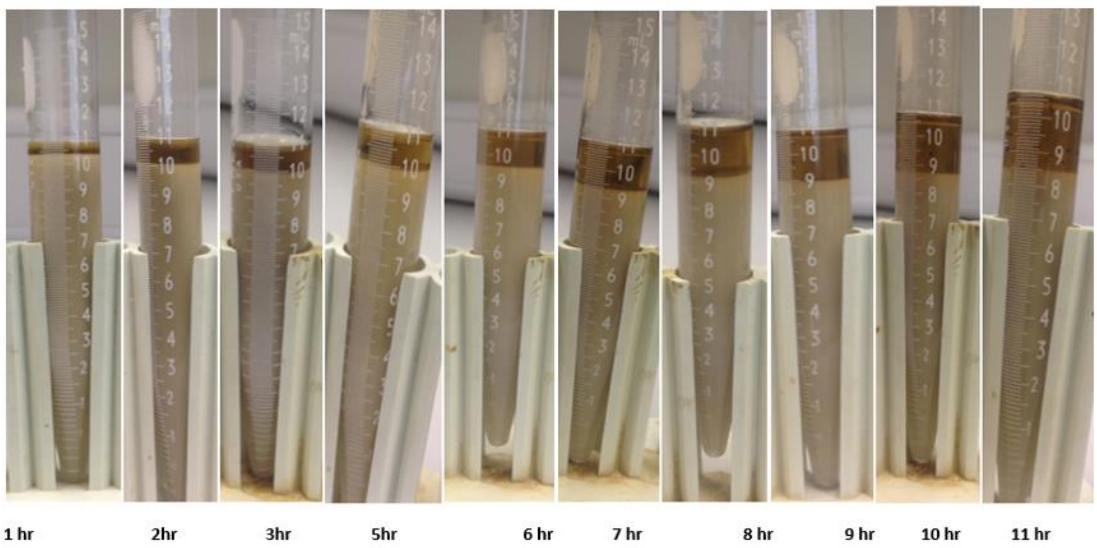

Figure 4.2 Diesel emulsified acid stability at 135°C

4.4 Pressure Drop Profiles

The pressure drop across the core during the injection of both diesel and waste oil emulsified acids at injection rates of 0.5, 2, 5 and 10 cc/min is shown in Fig. 4.3 and Fig. 4.4. All the core flood experiments conducted at 3000 psi back pressure and 135°. Fig. 4.3 illustrate the pressure drop profile for waste oil emulsified acid at lower injection rates. In Fig. 4.3 and Fig 4.4 the normal trend of the pressure drop profile existed for 2, 5 and 10 cc/min, the pressure drop initially was constant during the injection of de-ionized water. At the instant where emulsified acid injection started, the pressure drop initially slightly increased, then the pressure drop started to decrease as the emulsified acid penetrated deep into the core. The first increase in the pressure drop across the core can be referred to the high viscosity of emulsified acid injected into the core. As the calcite reacted with the emulsified acid, calcite dissolution started. At the same time, the calcite was reacting with emulsified acid, wormholes started to form and penetrate the core. These created wormholes caused the pressure drop to decrease. The increase, stabilization or decrease in pressure drop, depends mainly on the extent of dissolution in the length of the core. When the created wormholes extend from the core inlet face to the core outlet, an emulsified acid breakthrough occurs.

In Fig. 4.3 when waste oil emulsified acid was injected at 0.5 cc/min there was no breakthrough and the pressure was building up continuously due to the increase of fluid viscosity resulting from large amount of the reactant products, 0.78 pore volume of emulsified acid was injected then the experiment was stopped to prevent the sleeve and core damage. The injected acid was consumed in the wormhole enlargement instead of deep penetration. Also, in Fig. 4.4, the same trend for 0.5 cc/min of waste oil emulsified acid was observed, however, the breakthrough was achieved after a long time of injection.

In conclusion, waste oil and diesel emulsified acids presented an almost the same trend of pressure drop profiles with the slight difference only at 0.5 cc/min where waste oil emulsified acid didn’t breakthrough.

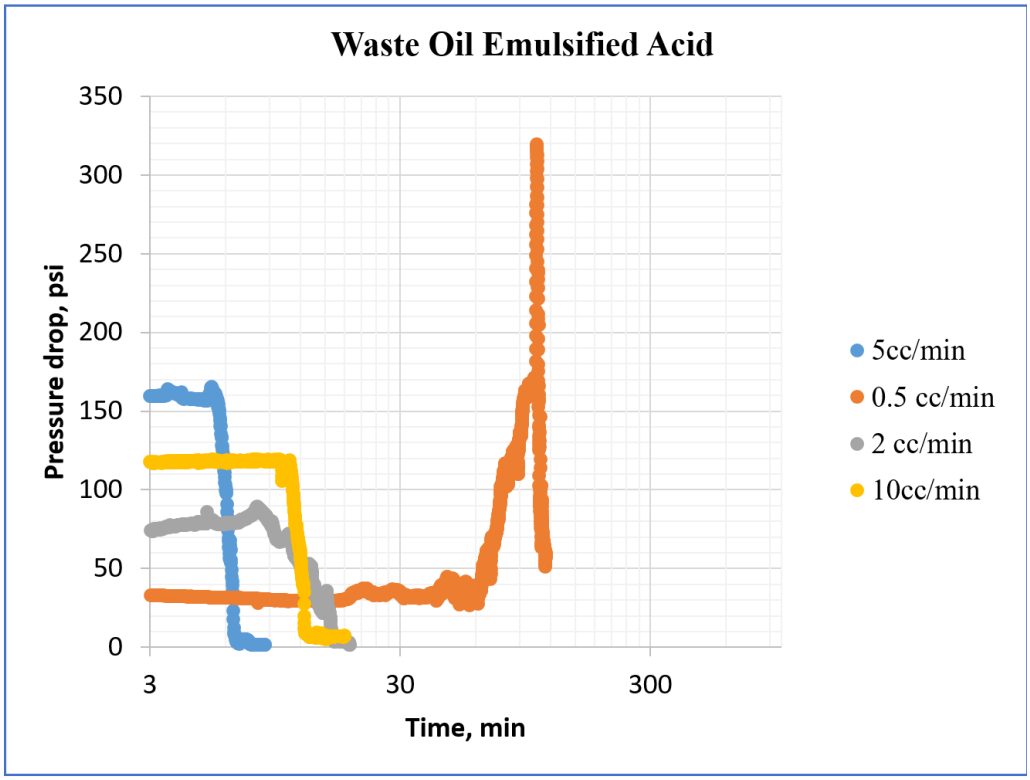

Figure 4.3 Pressure drop profile for waste oil emulsified acid coreflood experiments

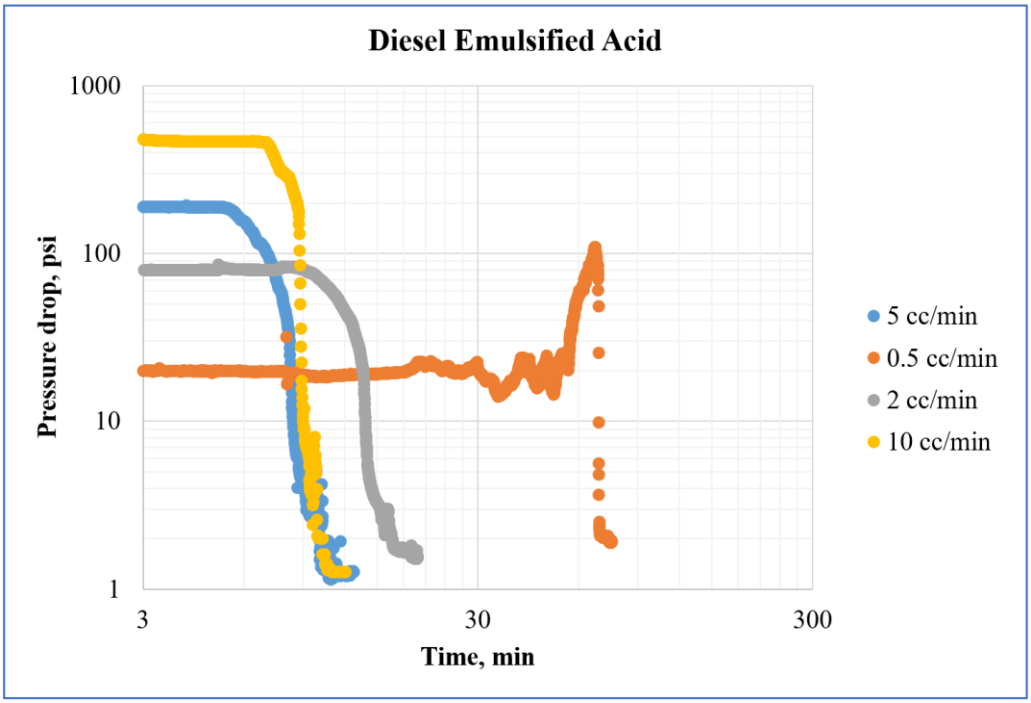

Figure 4.4 Pressure drop profile for diesel emulsified acid coreflood experiments

4.5 Optimum Injection Rate

The optimum injection rate for acidizing is the injection rate at which the least volume of acid (pore volumes) will be injected to achieve the breakthrough. In this study, acid was injected at four different rates under pressures of 3,000 psi and 135°C. The pore volumes required to breakthrough were plotted versus the flow rates of injection. This is a conventional plot that gives a u-shaped curve plot, which becomes a benchmark to measure the quality of any stimulation fluid, the lowest point on which being the optimum injection rate at the specific experimental condition. Eight Coreflood experiments were performed using an emulsified acid system. The first four is to study the new waste oil emulsified acid while the second four experiments used the conventional diesel emulsified acid for performance comparison. The volume of acid to achieve a breakthrough was a function of the acid injection rate. Fig. 4.5 compare, the relationship between the volume of acid to break through and emulsified acid injection rate, for the novel emulsified acid and two other systems of acid (Diesel emulsified acid and plain HCl). From Fig. 4.5, it is obvious that, for waste oil emulsified, as the injection rate increased, the volume of emulsified acid to breakthrough decreased and reached a minimum at 5.0 cc/min. For emulsified acid injection rates greater than 5 cc/min, the volume of emulsified acid to achieve breakthrough increased. This indicates that, for waste oil emulsified acid, the optimum injection rate was 5.0 cc/min.

In conclusion, the optimum pore volume to break through PVBT for waste oil was achieved at 5 cc/min while for conventional diesel emulsified acid was at 2 cc/min. For higher injection rate i.e. 5 and 10 cc/min, the novel emulsified acid exhibited the best performance among the three stimulation fluids whereas at lower ones the new acid system presented better efficiency than plain HCl and close to that of diesel. The optimum PVBT for waste oil was lower than the diesel one by almost half. Finally, it can be stated that the waste oil emulsified acid could

be used in the large window of injection rates (2-5 cc/min) since it has relatively lower PVBT compared to the other two stimulation fluids.

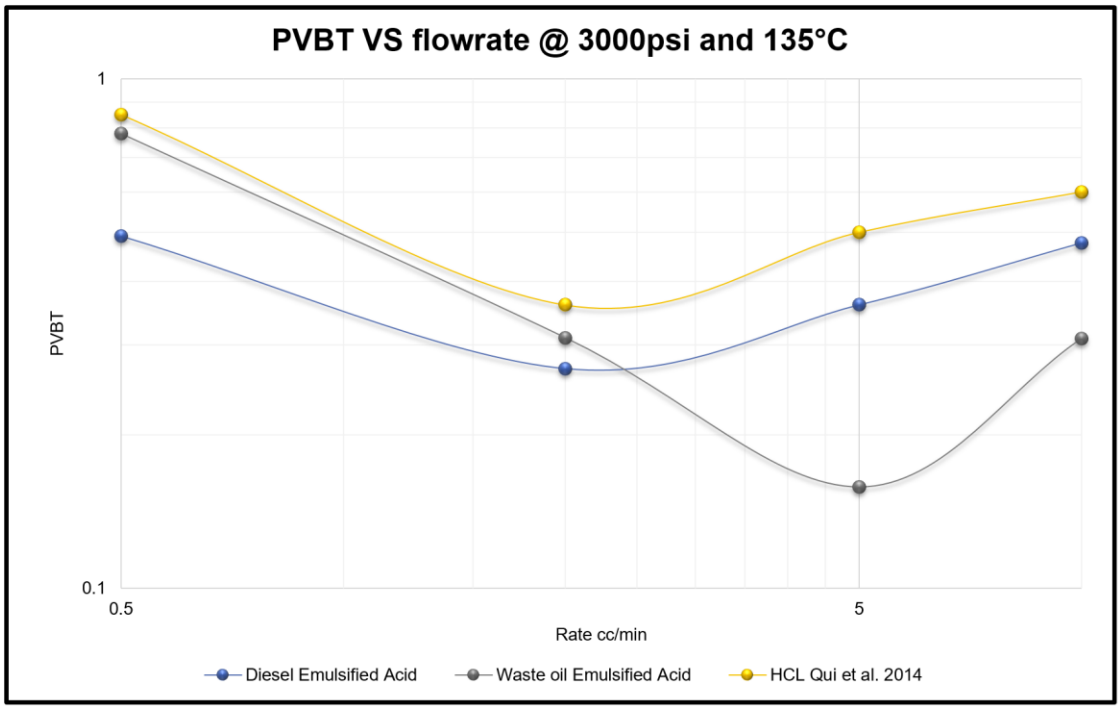

Figure 4.5 Pore volumes injected to achieve breakthrough at different injection rate

4.6 Inlet Face Image of the Cores

The shape of the core inlet face for each Coreflood experiment was captured and shown in Fig. 4.6. For 0.5 cc/min waste oil emulsified acid core flood the face inlet was bigger due to higher dissolution rate at the surface and this was confirmed also, through CT scan Fig. 4.7.

4.7 CT Scan for Acidized Cores

For better comprehension of the resulted wormhole characteristic form both stimulation fluids under investigation, the CT-scan image for the Indiana limestone cores after injection of both waste oil and diesel emulsified acids were taken and analyzed through Pregeos software. The 3D CT-scan image shown in Fig. 4.7 confirms both the pressure drop and the PVBT profiles. For instance, waste oil emulsified acid achieved the optimum injection rate at 5 cc/min, and from the Ct-scan we can see that a narrow and braches-free worm hole was created and lower acid was consumed to achieve this. This explanation is also valid for diesel emulsified acid at 2 cc/min. At extremely low rates, here is 0.5 cc/min, since the reaction rate is very fast and the mass transfer of hydrogen ions a limited phenomenon, the acid is consumed on the face of the core and wormhole enlargement instead of propagating forward. A dominant single hole is created if the injection rate is kept at it optimum. As the injection rate is further increased, though the volume required for breakthrough does not increase much, however, the structure of the dissolution pattern changes to unfavorable ramified structures instead of a single dominant hole as shown for diesel emulsified acid at 10 cc/min in Fig. 4.7. Wormhole volume fraction across the core profiles illustrated in Fig. 4.8 and Fig 4.9 was generated from the CT-scan image using the Pregeos software. The volume fraction calculated for each image of 1 mm thickness along the core. This also,

confirms the 3D ct-scan image as well as the PVBT curves. For example, at a lower injection rate of 0.5 cc/min, large wormholes were observed in the 3D image in Fig. 4.7 which can be confirmed in both Fig. 4.8 and Fig. 4.9 since the largest volume fraction was obtained at this rate compared to the other three injection rates.

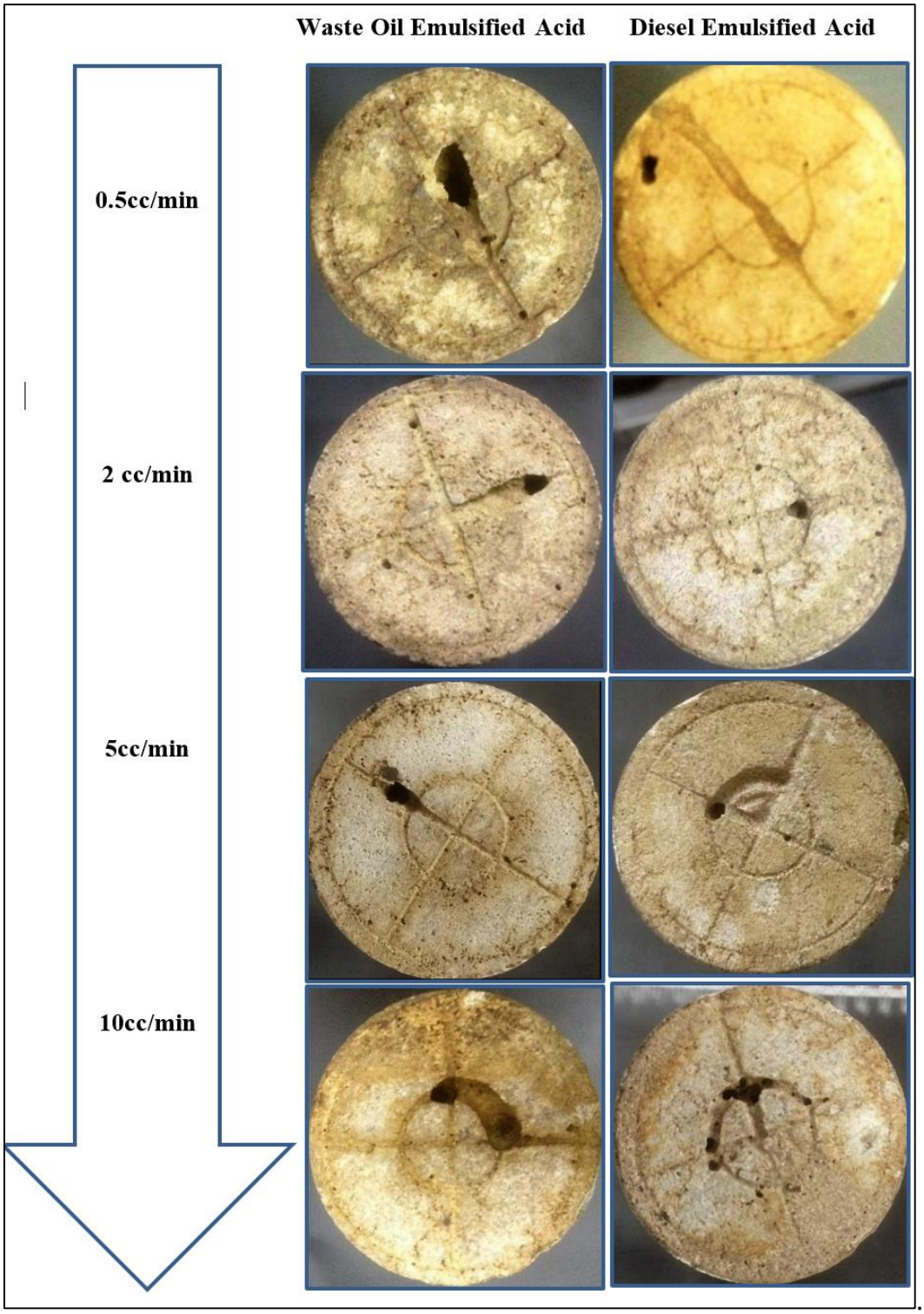

Figure 4.6 Inlet face images for all cores

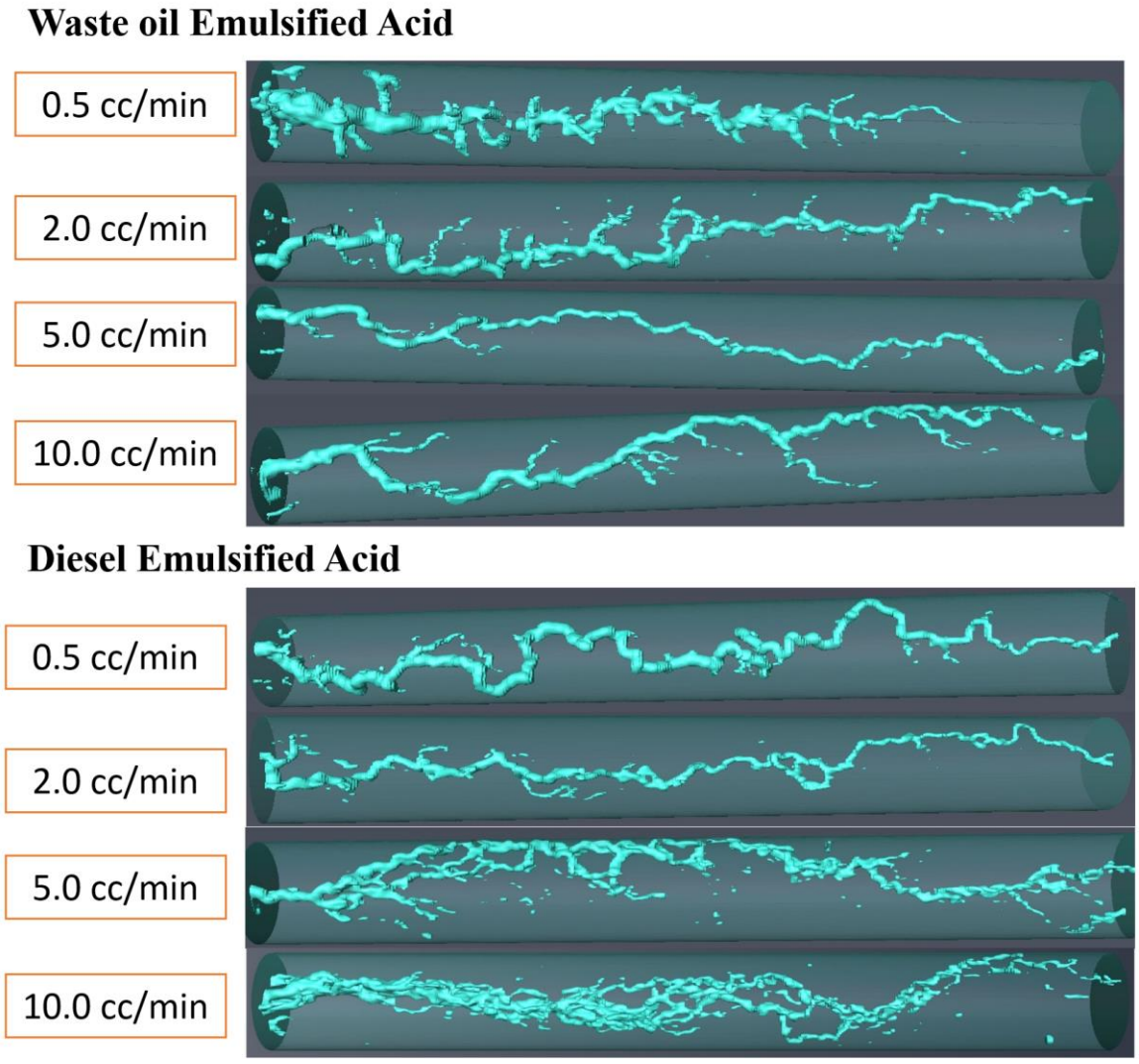

Figure 4.7 3D CT Scan for acidized cores analyzed through Pregeos software

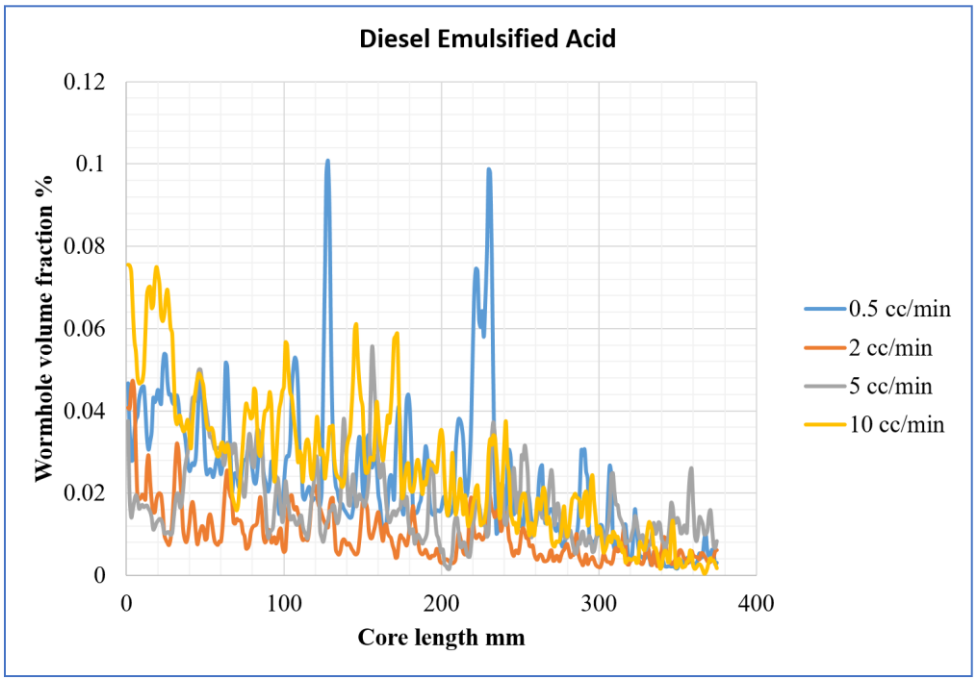

Figure 4. 8 Wormhole volume fraction along the core for diesel emulsified acid

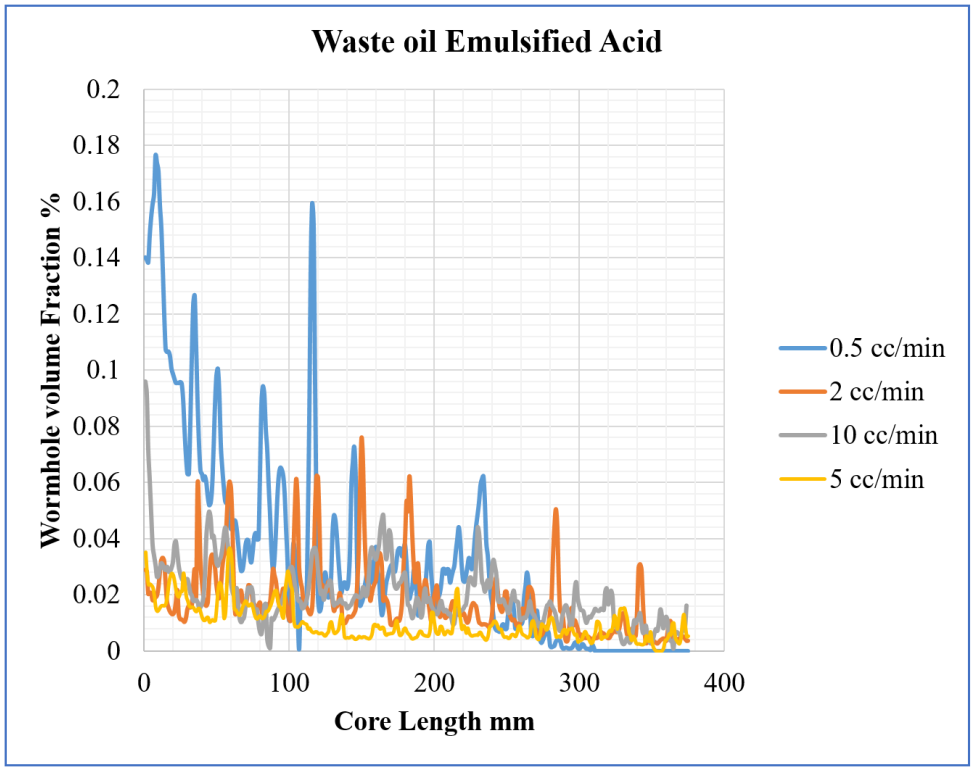

Figure 4. 9 Wormhole volume fraction along the core for waste oil emulsified acid

CHAPTER 5

Rotating Disk Experiment Results

The diffusion coefficient (D_e) that used in acid stimulation treatment modeling, for the conventional diesel, emulsified acid at deep down whole (high-pressure high-temperature) condition was not investigated. From an intensive literature review the maximum pressure and temperature that have been reported in diffusion coefficient calculation for emulsified acid were1100 psi and 110°C respectively (M. A. Sayed et al. 2012) which is extremely low to mimic the HPHT reservoir conditions. The values of D_e obtained at lower experimental conditions i.e (low-pressure, low-temperature) cannot be extrapolated to HPHT condition, because at HPHT most of CO2 prefer to stay in the aqueous phase, and eventually yield to a lower D_e as observed by (Khalid, Sultan, and Qiu 2015). Also, very limited work was done to study the effect of oil saturation on the emulsified acid reaction kinetics. Hence, in this work series of reaction kinetics were done using rotating desk instrument to study two objectives, Firstly, to calculate the reaction rate and the diffusivity D_e of the conventional emulsified acid at deep reservoir condition i.e. 135°C and 3000 psi. The second thing was to study the effect of crude oil saturation on both reaction rate and emulsified acid diffusivity at the same HPHT condition.

5.1 XRD and XRF Analysis of Calcite Core

To determine the mineralogy and the purity of calcite X-ray diffraction analysis was done. The XRD results showed that the core contains more than 98% calcite 1% dolomite and

less than 1% traces of quartz. Fig. 5.1 shows the profile of conducted XRD measurement in term of intensity versus 2-theta.

For further investigation and to be sure that there is no magnesium or dolomite in our disk samples X-ray elemental analysis was conducted. The XRF result shows that there is no trace of magnesium in our samples. These results are illustrated in table 5.1.

Table 5. 1 XRF results

Elements	Norm. Int.	Concentration %
Al	26.4713	0.579
Si	40.554	0.3369
P	119.1805	0.3752
K	195.8076	0.0584
Ca	214962.3449	65.94
Fe	244.3066	0.1597
Oxides	Norm. Int.	Concentration %
Al2O3	26.4713	1.095
SiO2	40.554	0.721
P2O5	119.1805	0.8598
K2O	195.8076	0.0704
CaO	214962.3449	92.26
Fe2O3	244.3066	0.2284

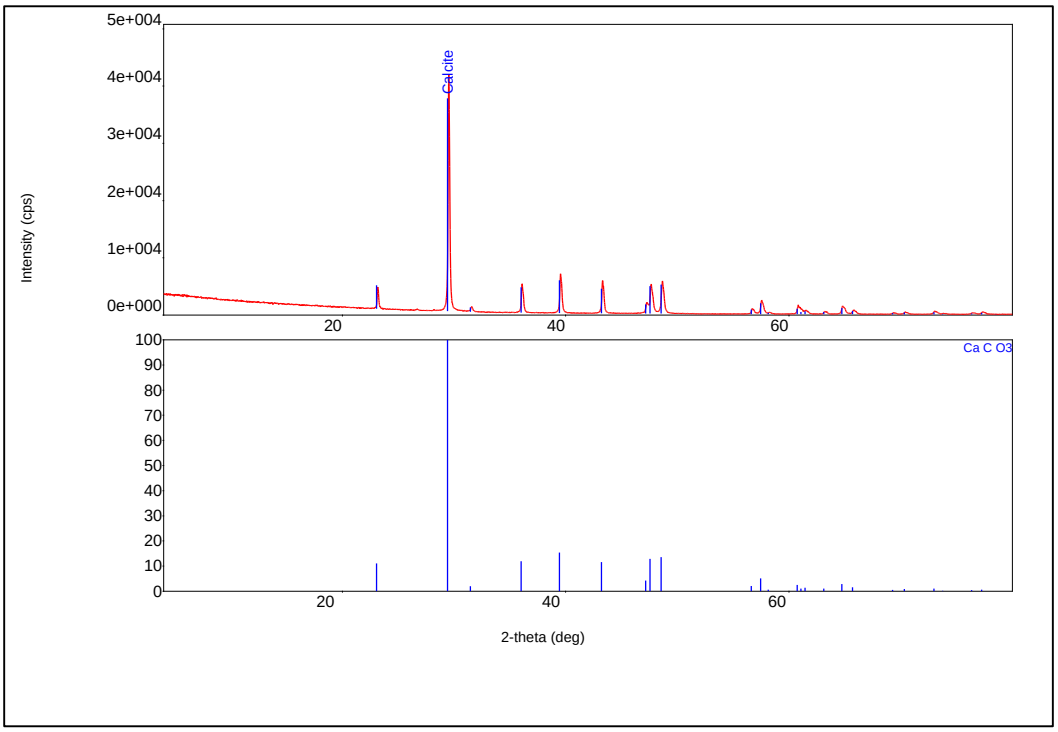

Figure 5.1 XRD results for calcite disks used in this study

5.2 Viscosity of Emulsified Acids at a Temperature of 135°C

(S. Al-Mutairi et al. 2009) conclude that emulsified acid is a non-Newtonian shear thinning fluid and its rheological parameters are necessary for determining the diffusivity of the acid. The apparent viscosity of the diesel emulsified acid was measured at shear rates up to 1000 s^{-1} at different temperature 25, 60, 100°C this was done by (Sidaoui and Sultan 2016). The power low model parameters calculated by generating correlation from the data obtained at these temperatures Then the correlation was used to get the rheological parameters at 135°C.Results were shown Fig. 5.2. Fig. 5.3. Table 5.2 shows the values of n and K at different temperature for the emulsified acid.

Table 5. 2 Power-low values at different temperature for the emulsified acid

Temperature ˚C	Power Law Constant, K (mPa.s^n)	Power Law Index, n	Correlating Coefficient, R^2
25	1064.9	0.53	0.96
60	660.9	0.578	0.983
100	440.1	0.612	0.993

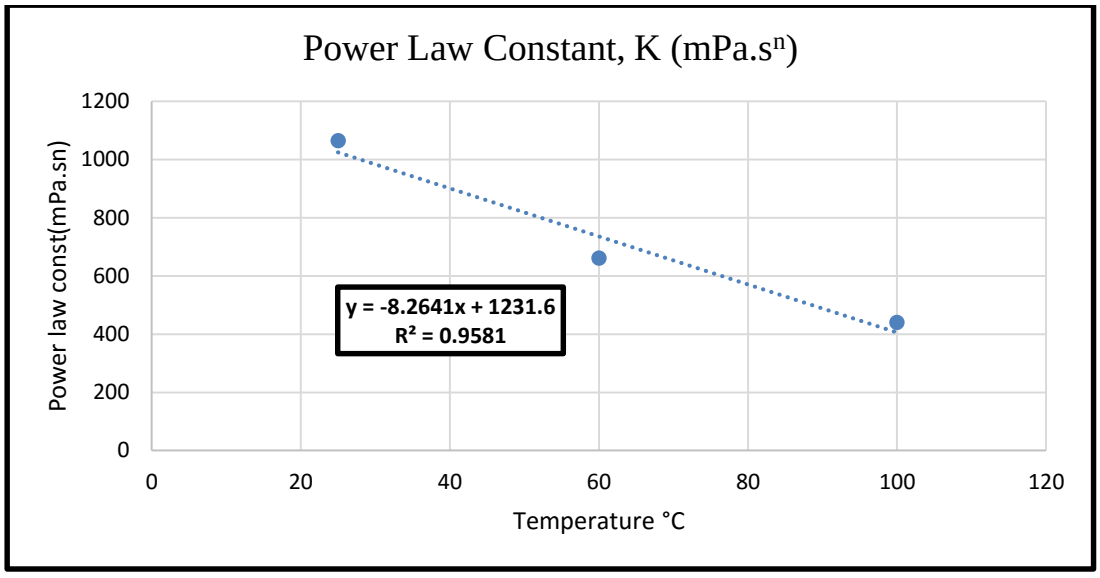

Figure 5.2 The power low constant correlation with temperature

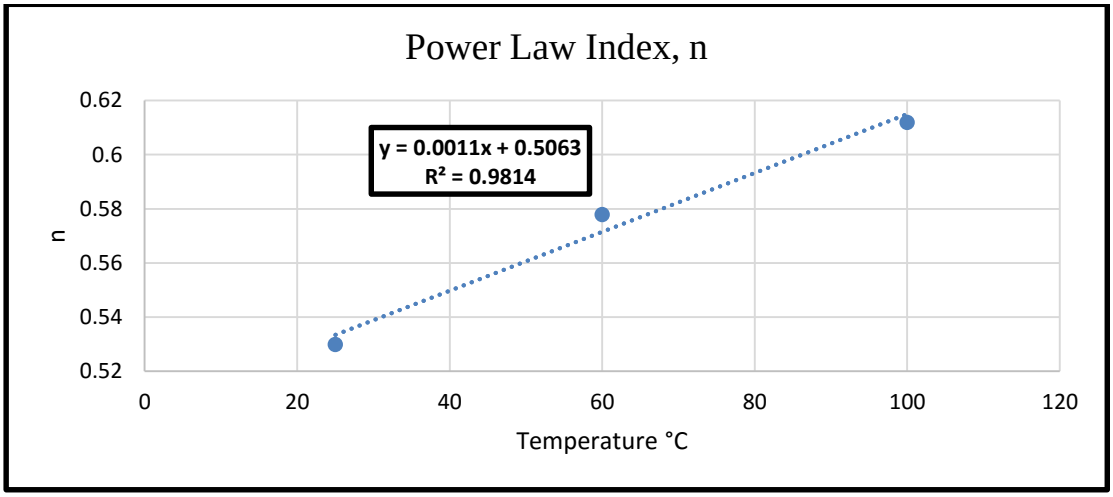

Figure 5.3 The power low index correlation with temperature

5.3 Stability of Emulsified Acids at a Temperature of 135°C

The knowledge of emulsion thermal stability is important in the application of emulsified acids. The emulsified acid should reach the formation breaking into phases. To make this to occur, the emulsified acid should survive the high temperature, high shearing in the tubing, and the high pressure at the downhole condition, for the minimum time that grants it to interaction the formation. One simple and quick method to determine the stability is to observe phase separation for emulsion component with time at required temp. This method was adopted and applied using see through the oven. Fig 5.4 illustrates that the emulsified acid used in this study was stable for more than 11 hours. In Fig. 5.5 the fraction of the volume of the emulsion remaining with time at 135°C.

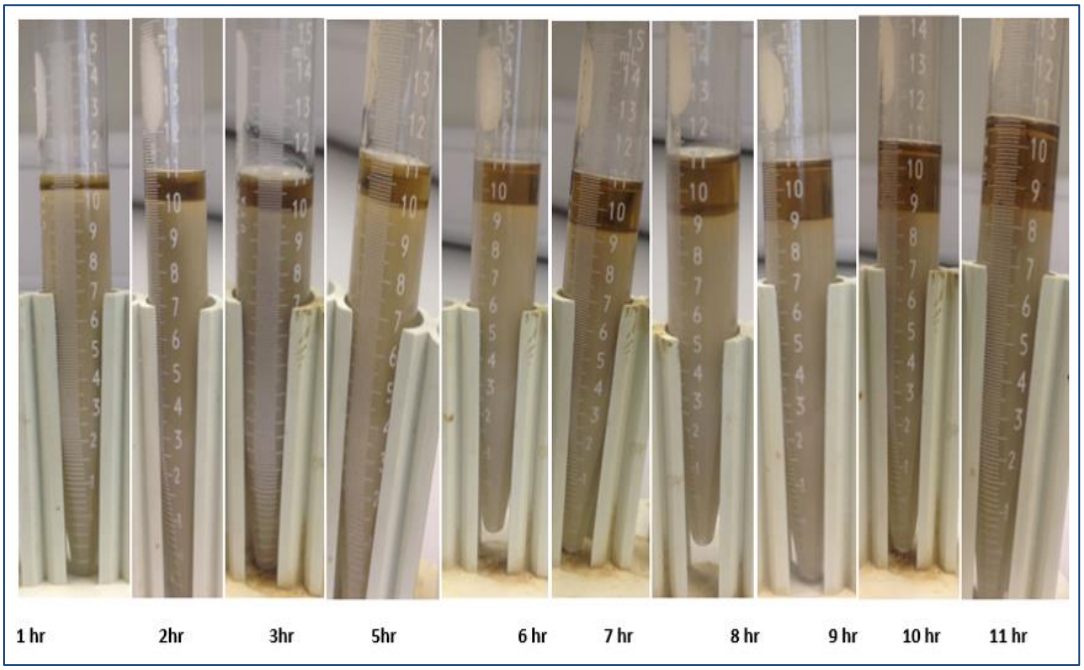

Figure 5.4 Stability of Emulsified Acids at a temperature of 135°C

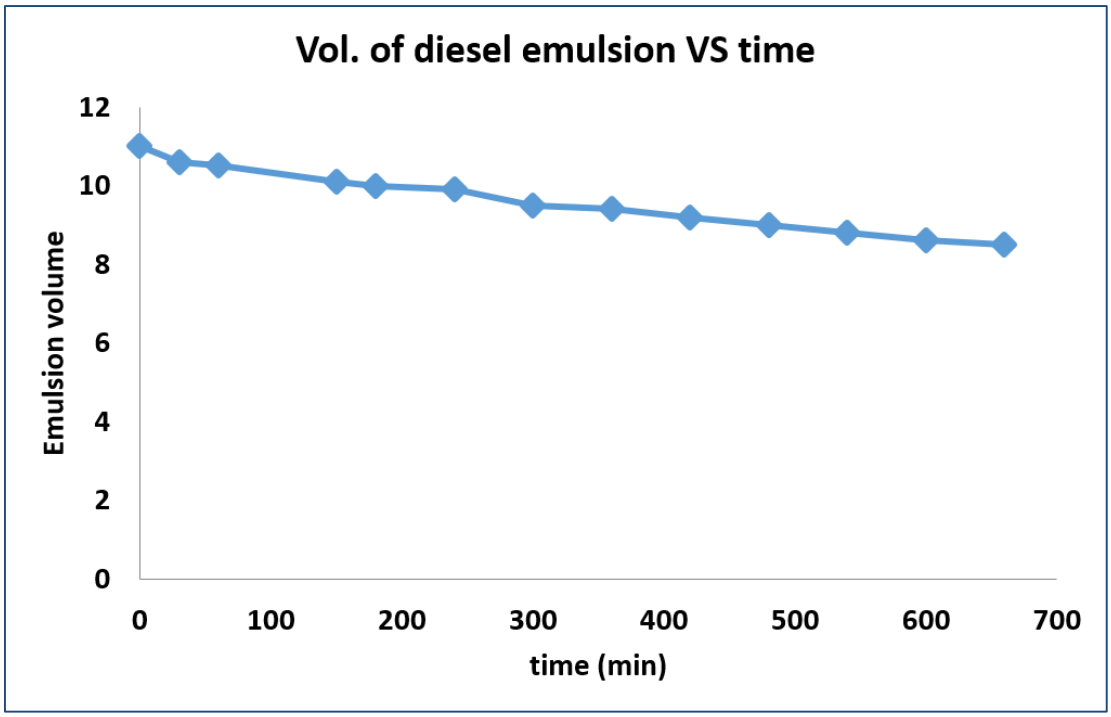

Figure 5.5 Stability of Emulsified Acids at a temperature of 135°C

5.4 Reaction of Emulsified Acid and Limestone

The reaction kinetics through rotating disk experiments that performed at a high-temperature and high-pressure of 135°C and 3000 psi respectively, to ensure that CO2 will remain in solution as suggested by(Khalid, Sultan, and Qiu 2015). Experiments were performed using low permeability and porosity limestone core plugs. The rotational speeds where experiments were performed were from 200 and up to 1500 rpm. Samples of 4 ml were withdrawn from the reactor each 2 minute. Ten fluid samples were collected in each experiment, and the analyzed through ICP-OES for calcium concentration. All experiments were performed for a 28 wt. % HCl acid to diesel ratio of 70:30 and emulsifier concentration of 1 vol. %. Table 5.3 and Table 5.4 revealed the experimental conditions for both dry and oil saturated limestone respectively.

Table 5. 3 Set # 1 Experiment Parameters

Experiment Parameters Set # 1	
Rock Type	Calcite
Core Type	Local outcrop
Temperature, °C	135
Pressure, psi	3000
Fluid	Diesel Emulsified Acid
HCL concentration wt.%	28
Disk Rotational speeds, RPM	200, 400, 600, 1000, 1500

Table 5. 4 Set # 2 Experiment Parameters

Experiment Parameters Set # 2	
Rock Type	Calcite
Core Type	Local outcrop
Disk type	Oil saturated disk
Temperature, °C	135
Pressure, psi	3000
Fluid	Diesel Emulsified Acid
HCL concentration wt.%	28
Disk Rotational speeds, RPM	200, 400, 600, 1000, 1500

5.5 Emulsified Acid - Limestone Surface Reaction Pattern

The reaction rate and reaction patterns for limestone core samples with emulsified acids were studied using a rotating disk apparatus. The effect of the rotational speed on the dissolution pattern on the surface of the disk, at different rotational speeds from 200and up to 1500 rpm and at135°C, is presented in Fig. 5.6. It has shown that at 200 rpm, the disk relatively remained uniform, and the dissolution rate was very low which indicates small rock/acid reaction. As the RPM increased to 1500, the dissolution increased and the surface of the rock was greatly changed.

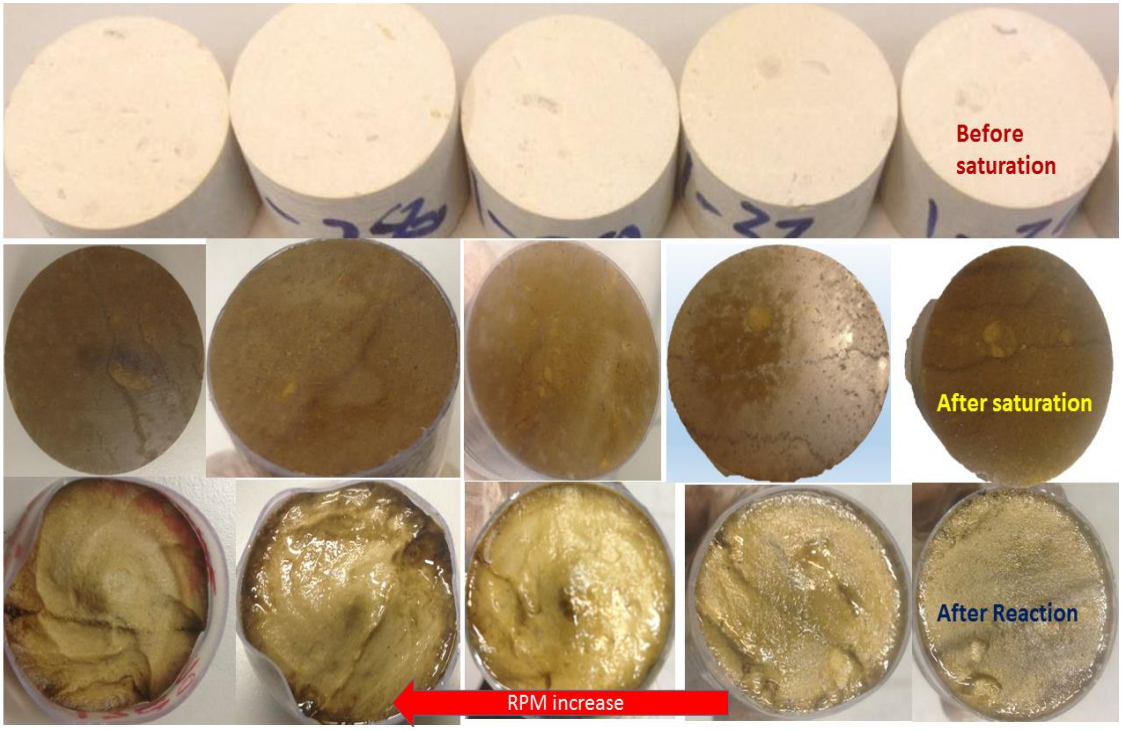

Figure 5.6 Emulsified acid - limestone surface reaction pattern

5.6 Calculation of Emulsified Acid- Limestone Dissolution Rate:

All the experiments, for both dry and crude oil, saturated limestone disks, were performed at 3000 psi and 135°C with disk rotational speeds up to 1500 rpm. The emulsified acid was prepared so that the final acid concentration was 28 wt. % HCl and the acid volume fraction (ϕ) was 0.7. Samples were taken automatically from the reactor every 2 minutes for 20 minutes. The calcium concentration, in every sample, was measured using the ICP-OES (Inductively Coupled Plasma). The concentration was plotted as a function of time. The dissolution rate is then calculated by dividing the slope of the best fit straight line by the initial surface area of the disk.

Fig. 5.7 and Fig. 5.8 show the change in concentration of calcium as a function of reaction time for reaction with dry and crude oil saturated disks respectively. From those plots, the calcium concentration increased, as the disk rotational speed increased, the plotted data points were fitted with a straight line and the slope of this line was used to calculate the dissolution rate at each rpm.

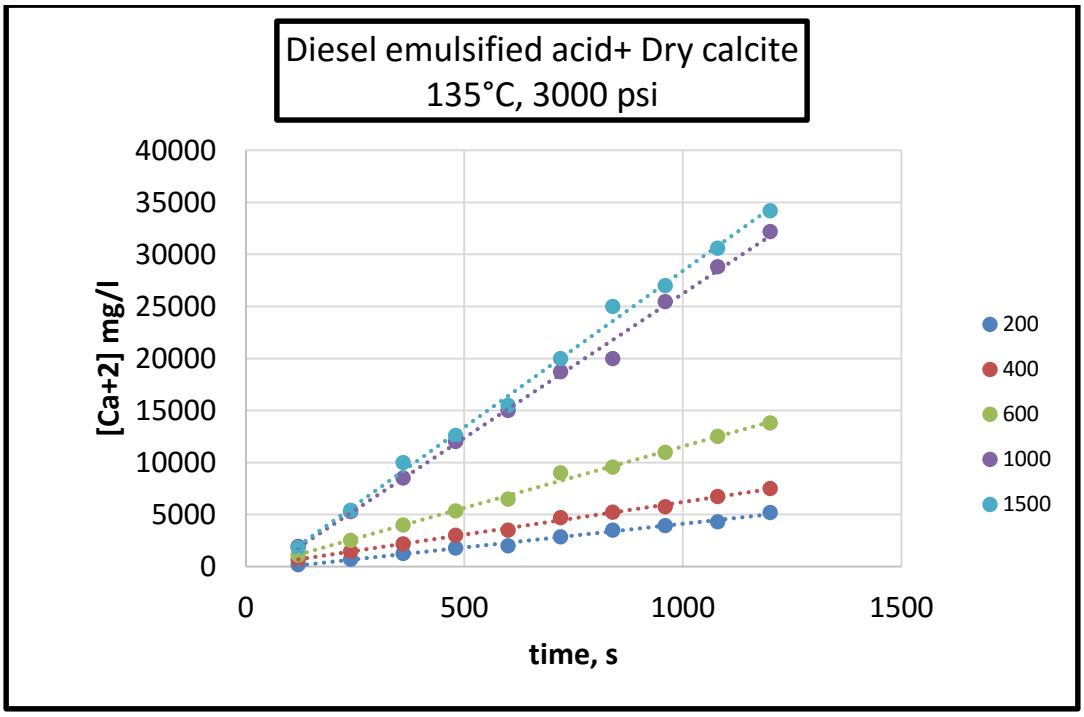

Figure 5.7 Calcium concentration with time for dry limestone reaction kinetic at different RPM

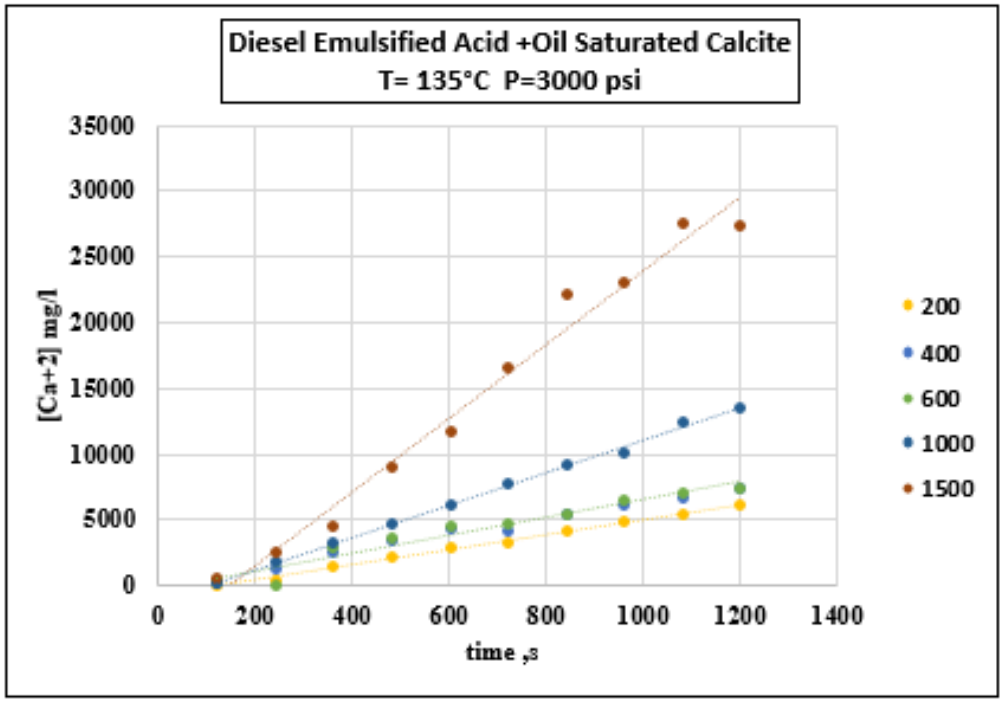

Figure 5.8 Calcium concentration with time for crude oil saturated limestone at different rpm.

When the mass transfer limited regime is predominating, the reaction rate can be directly measured from the mass flux. The plot of the dissolution rate values against the desk rotational speeds to the power (1/(1+n)), where n is the power law index obtained from the rheological properties measurements, in this work we used correlation, is used in defining the boundary between the mass transfer limited regime and the surface reaction limited regime. Fig. 5.9 shows the reaction rate versus disk rotational speed to the power 1/(1+n) for Acid/dry and acid/crude oil saturated limestone reaction respectively. It is obvious that, at 135°F, the reaction of diesel emulsified acid with dry calcite was mass transfer limited at lower RPM and surface reaction limited at rpm above 1000.On the other hand, the reaction of diesel emulsified acid with oil saturated calcite was found to be mass transfer limited even at higher RPM 1000,1500.

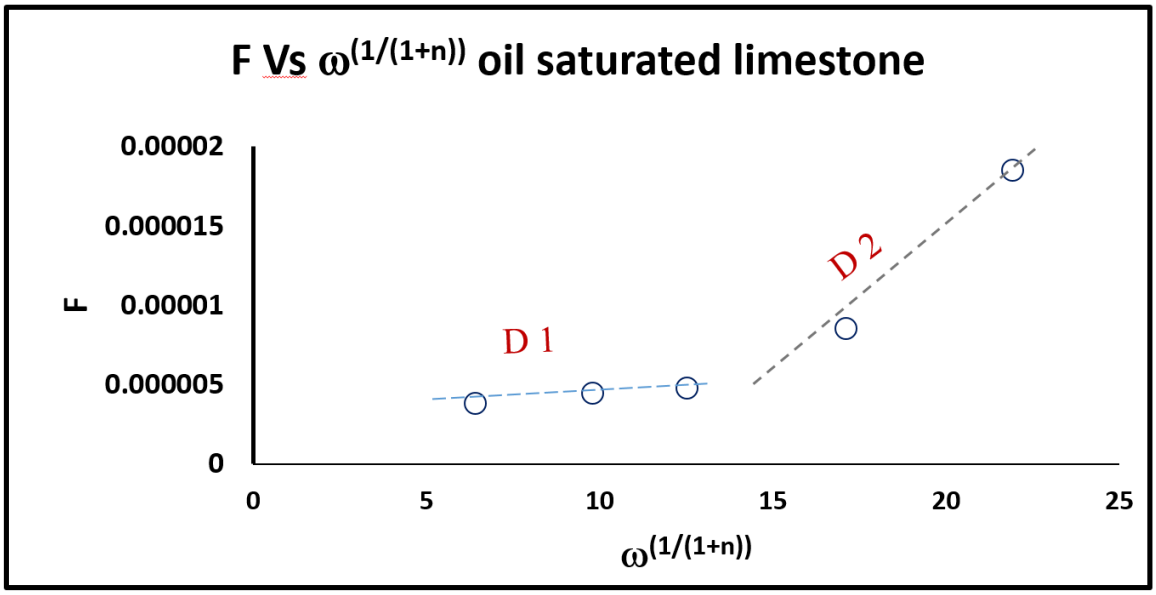

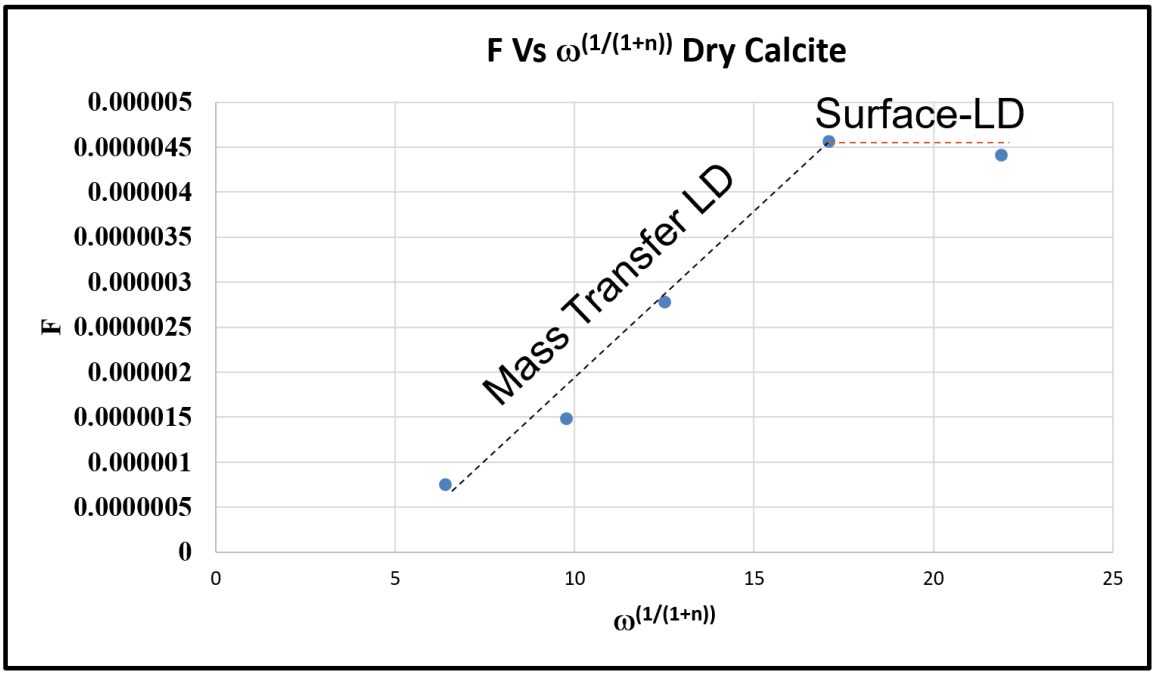

Figure 5.9 The F-function versus disk rotational speed to the power 1/(1+n)

5.7 Diffusion Coefficient of Emulsified Acid with Dry and Oil Saturated Limestone.

Table 5-5 shows the values for the function $\emptyset(n)$ at different power-law indices, introduced by (Hansford et al.1968).From the rheological study, values of k, n, and $\emptyset(n)$ were determined at 135°C. From The plot of F function versus $\omega^{1.5}$ the slope will be the value of A. From the definition of "A" parameter in the equation 6.1, the diffusion coefficient can be estimated for each emulsified acid-rock system. Table 5.6 summarizes estimated diffusion coefficient as well as typical values from the literature.

Two regions of diffusion coefficient in the reaction with oil saturated calcite disks was observed. At lower rpm generally, the reaction rate is slow and the reaction occurs in a very thin external layer of the disk, where high oil saturation exists, which acts as an additional barrier for H^+ to reach the rock surface and eventually retard the reaction and yield to a lower De. Whereas at higher RPM the value of the D_e was almost more than double and that mainly because the external oil saturated layer is consumed due to the rapid reaction and more reaction take place as if the rock was dry.

$$\boldsymbol{J_{Ca+2} = \left[\emptyset(n)\left(\frac{K}{\rho}\right)^{-1/(3(n+1))} r^{(1-n)/3(n+1)} \omega^{1/(1+n)} D^{2/3}\right] c_0 = A\omega^{1/(1+n)}} \ldots\ldots. \text{(6-1)}$$

Table 5. 5 The values for the function $\emptyset(n)$ at different power-law indices

n	0.2	0.4	0.6	0.8	1	1.3
$\emptyset(n)$	0.695	0.662	0.655	0.647	0.633	0.618

For oil saturated limestone reaction kinetics at lower rpm, the D_{e1} was 3.16228E-11 cm^2/s where at higher ones the D_{e2} value reported was 4.64758E-10 cm^2/s. On the other side, for dry limestone, the D_e value obtained was almost double the average of D_{e1} and D_{e2}.

The values of D_e at HPHT was much lower than those obtained at the relatively low-pressure low-temperature condition. For instance, (S. Al-Mutairi et al. 2009) studied the reaction kinetics of diesel emulsified acid at 110°C and 1100 psi at same emulsifier concentration that used in the current study 1 vol%, He reported D_e value of 2.430E-07 cm^2/s. Also, at similar conditions and with only different of emulsifier type Syed 2012 (M. A. Sayed et al. 2012) reported a higher value of D_e 5.093E-09 cm^2/s. For extremely low temperature (Rozieres, Chang, and Sullivan 1994) reported an effective diffusion coefficient of 2.64 E-08 cm^2/s for the emulsified acid at 28.3°C.

To sum up, two conclusions can be drawn from the above discussions, firstly the D_e value at HPHT is much lower than those obtained at LPLT. The extrapolation of these D_e values at lower down hole conditions for deep reservoirs could lead to severe acidizing and hydraulic fracturing design inaccuracy. Secondly, two D_e values were reported for oil saturated limestone reaction kinetics and this mainly because of crude oil saturation effect.

CHAPTER 6

CONCLUSIONS AND RECOMMENDATIONS

Conclusions

- The new waste oil emulsified acid cost was reduced Further introducing special nanoparticles as emulsion stabilizer instead of surfactants.
- The new emulsion has the stability of more than 5 hours at 135°C.
- The performance of the new emulsified acid system in stimulating deep limestone reservoir i.e. HPHT was investigated, and compared with conventional diesel emulsified acid one through Coreflood experiments.
- The optimum pore volume to break through PVBT for waste oil emulsified acid was achieved at 5cc/min while for conventional diesel emulsified acid was at 2 cc/min
- At 2 cc/min, the new emulsified acid showed almost close PVBT for diesel-emulsion which indicate the same performance of diesel can be achieved using the emulsion.
- The optimum PVBT for waste oil was lower than the diesel one by almost half.
- Waste oil emulsified acid could be used in the large window of injection rates (2-5 cc/min) from core-flow experiments, however higher injection rate are not achievable in field operation especially for emulsified acid as high viscous fluid.

- From face inlet and CT-scan, No face dissolution was noticed in the core inlet face for all the injection rates studied.
- lab experiments showed a good potential for the waste-oil emulsion to be used in the oil field stimulation.
- The reaction of diesel emulsified acid with dry calcite was found to be mass transfer limited at lower RPM and surface reaction limited at rpm above 1000.
- The reaction of diesel emulsified acid with oil saturated calcite was to be mass transfer limited even at higher RPM 1000,1500.
- Two regions of diffusion coefficient in the reaction with oil saturated calcite disks was observed. At lower rpm generally, the reaction rate is slow and the reaction occurs in a very thin external layer of the disk, where high oil saturation exists, which acts as an additional barrier for H^+ to reach the rock surface and eventually retard the reaction and yield to a lower De. Whereas at higher RPM the value of the D_e was almost more than double and that mainly because the external oil saturated layer is consumed due to the rapid reaction and more reaction take place as if the rock was dry.

Recommendations

1. The rheology of the new emulsified acid should be measured at 135°C instead of using correlation for better accuracy when calculating the diffusion coefficient.

2. Corrosion inhibitor and Iron control agents should be added in the emulsion to prevent the corrosion in lab instrument i.e. (RDA, Coreflood, shafts, etc.) as well as the tubing system when used for field applications.
3. A five RDA experiments for the new waste oil emulsified acid could be done to determine its dissolution rate and the diffusion coefficient with limestone.
4. Reaction kinetics experiment could be carried out to study the performance of the new emulsified acid for dolomitic reservoirs.
5. A study on the sensitivity of the emulsion to changes in the input oil
6. Preferably the development of electrical or optical scattering techniques for monitoring the emulsion stability/breakdown in more efficient and deterministic fashion.
7. Cost/Benefit analysis for waste oil emulsified as a new stimulation fluid product.

References

Adenuga, O.O., M.A. Sayed, and H.A. Nasr-El-Din. 2013. “Reactions of Simple Organic Acids and Chelating Agents with Dolomite.” *Society of Petroleum Engineers Journal*, no. March: 1–15.

Al-douri, Ahmad F, M A Sayed, A Texas, Carl Aften, and P F P Technology. 2013. “SPE 164110 A New Organic Acid to Stimulate Deep Wells in Carbonate Reservoirs,” 1–17.

Al-Mutairi, S H, A D Hill, and H A Nasr-El-Din. 2007. “SPE 107741 Effect of Droplet Size , Emulsifier Concentration , and Acid Volume Fraction on the Rheological Properties and Stability of Emulsified Acids,” no. 1: 1–16.

Al-Mutairi, S H, A D Hill, H A Nasr-El-Din, and A D Al-Aamri. 2008. “SPE 112454 Effect of Droplet Size on the Reaction Kinetics of Emulsified Acid With Calcite.”

Al-Mutairi, Saleh, Hisham Nasr-El-Din, Alfred Hill, and Ali Al-Aamri. 2009. “Effect of Droplet Size on the Reaction Kinetics of Emulsified Acid With Calcite.” *SPE Journal* 14 (4): 606–16. doi:10.2118/112454-PA.

Buijse, M A, and M S Van Domelen. 2000. “Novel Application of Emulsified Acids to Matrix Stimulation of Heterogeneous Formations,” no. August 1999.

De Groote, Melvin. 1933. Process For Increasing The Output Of Oil Wells. 1922154, issued 1933.

Economides, Michael J, and Kenneth G Nolte. 1989. *Reservoir Stimulation, 2nd Edition*. Englewood Cliffs, New Jersy, USA: Prentice Hall.

Hansford, Geoffrey S., and Mitchell Litt. 1968. “Mass Transport from a Rotating Disk into Power-Law Liquids.” *Chemical Engineering Science* 23 (8): 849–64. doi:10.1016/0009-2509(68)80020-X.

Kalfayan, Leonard. 2008. *Production Enhancement with Acid Stimulation, 2nd Edition*. PennWell.

Kasza, P, Gas Inst, M Dziadkiewicz, Polish Oil, Gas Co, M Czupski, and Gas Inst. 2006. "SPE 98261 From Laboratory Research to Successful Practice : A Case Study of Carbonate Formation Emulsified Acid Treatments."

Khalid, Muhammad Ali, Abdullah Sultan, and Xiangdong Qiu. 2015. "Revisiting Reaction Kinetics and Diffusion Rate of Dolomitic Rock with HCl." *SPE North Africa Technical Conference and Exhibition*.

Lund, Kasper, H. Scott Fogler, and C. C. McCune. 1973. "Acidization-I. The Dissolution of Dolomite in Hydrochloric Acid." *Chemical Engineering Science* 28 (3): 691–700. doi:10.1016/0009-2509(77)80003-1.

Lund, Kasper, H.S. Fogler, C.C. McCune, and J.W. Ault. 1975. "Acidization—II. The Dissolution of Calcite in Hydrochloric Acid." *Chemical Engineering Science* 30 (8): 825–35. doi:10.1016/0009-2509(75)80047-9.

Nasr-El-Din, Hisham A., and Abdullah Mohammed Al-Mohammed. 2006. "Reaction of Calcite With Surfactant-Based Acids." In *SPE Annual Technical Conference and Exhibition*, 1–14. Society of Petroleum Engineers. doi:10.2118/102838-MS.

Nasr-El-Din, Hisham A., Abdullah Mohammed Al-Mohammed, Ali Al-Aamri, and Omar A. Al-Fuwaires. 2006. "Reaction Kinetics of Gelled Acids with Calcite." In *International Oil & Gas Conference and Exhibition in China*, 5–7. Society of Petroleum Engineers. doi:10.2118/103979-MS.

Qiu, Xiangdong, Muhammad Ali Khalid, Abullah Sultan, and King Fahd. 2015. "How to Determine True Acid Diffusion Coefficient to Optimize Formation Damage Treatment ?"

Rabie, A I, A M Gomaa, All Spe, and A Texas. 2010. "Determination of Reaction Rate of In-Situ Gelled Acids With Calcite Using the Rotating Disk Apparatus," no. 1999.

Rabie, Ahmed I, Ahmed M Gomaa, Hisham A Nasr-el-din, A Texas, and All S P E Members. 2011. "SPE 140138 HCl-Formic In-Situ Gelled Acid for Carbonate Acidizing : Core Flood and Reaction Rate Study," no. 1978: 1–20.

Rozieres, John De, F. F. Chang, and R. B. Sullivan. 1994. "Measuring Diffusion Coefficients in Acid Fracturing Fluids and Their Application to Gelled and Emulsified Acids." *Proceedings of SPE Annual Technical Conference and Exhibition*. doi:10.2118/28552-MS.

Sayed, M. A., H. A. Nasr-El-Din, J. Zhou, S. Holt, and H. Al-Malki. 2012. “A New Emulsified Acid to Stimulate Deep Wells in Carbonate Reservoirs.” *Proceedings - SPE International Symposium on Formation Damage Control* 1 (1933): 254–79. http://www.scopus.com/inward/record.url?eid=2-s2.0-84861394136&partnerID=tZOtx3y1.

Sayed, M A, and H Nasrabadi. 2013. “Reaction of Emulsified Acids With Dolomite.” *Jcpt* 52 (May): 164–75.

Sayed, M a, a Texas, C a De Wolf, and All S P E Members. 2013. “SPE 165120 Emulsified Chelating Agent : Evaluation of an Innovative Technique for High Temperature Stimulation Treatments.”

Schechter, Robert S. 1992. *Oil Well Stimulation*. Englewood Cliffs, New Jersy, USA: Prentice Hall.

Sidaoui, Ziad, and Abdullah S Sultan. 2016. “Formulating a Stable Emulsified Acid at High Temperatures : Stability and Rheology Study.” In .

Sidaoui, Ziad, Abdullah S. Sultan, and Dominic Brady. 2017. “A Novel Approach to Formulation of Emulsified Acid Using Waste Oil.” *SPE Kingdom of Saudi Arabia Annual Technical Symposium and Exhibition*. doi:10.2118/188116-MS.

Sidaoui, Ziad, Abdullah S Sultan, King Fahd, and Xiangdong Qiu. 2016. “Viscoelastic Properties of Novel Emulsified Acid Using Waste Oil : Effect of Emulsifier Concentration , Mixing Speed and Temperature.”

Taylor, K., a. Al-Ghamdi, and H. Nasr-El-Din. 2003. “Measurement of Acid Reaction Rates of a Deep Dolomitic Gas Reservoir.” *Proceedings of Canadian International Petroleum Conference*, no. 4: 49–56. doi:10.2118/2003-068.

Taylor, K C, S Mehta, and Saudi Aramco. 2006. “SPE 89417 Anomalous Acid Reaction Rates in Carbonate Reservoir Rocks.” *SPE Journal*, no. January 2004: 1–17.

Zhang, Wei, and Dennis P. Curran. 2006. “Synthetic Applications of Fluorous Solid-Phase Extraction (F-SPE).” *Tetrahedron* 62 (777): 11837–65. doi:10.1016/j.tet.2006.08.051.

Vitae

Name :Musa Eltayeb Musa Ahmed

Nationality :Sudanese

Date of Birth :5/3/1990

Email :musa277@gmail.com

Address :House no. 428,20 street , Alslama, Khartoum, Sudan

Academic Background :, MSc in petroleum engineering with distinctions grade from King Fahd University of Petroleum and Minerals 2017,

BSc in petroleum engineering, with first honors from University of Khartoum, 2013